INTRINSIC *UBV* COLORS OF RR LYRAE STARS*

CONRAD STURCH†

Lick Observatory, University of California, Mount Hamilton, California

Received May 17, 1965; revised September 20, 1965

ABSTRACT

Photoelectric observations on the *UBV* system of more than one hundred Bailey type *a*, *b* RR Lyrae stars were obtained to investigate the color indices near minimum light. It is shown that for most purposes of galactic research $B - V$ and $U - B$ may be treated as constant in the phase interval $0.5 < \phi < 0.8$. The $U - B$ index during this interval is correlated with the metallic-line blanketing derived from high-dispersion spectrograms, and is used to find a line-free index, $(B - V)_c$. A period versus $(B - V)_c$ relation is found for those variables in the galactic caps and, combined with observations from stars at lower latitudes, is used to obtain a cosecant reddening law. A $B - V$ excess at the poles of 0.03 mag. is adopted. From this, intrinsic *UBV* colors and individual color excesses are derived for the RR Lyrae stars. The probable error of an intrinsic color is only 0.01 mag. Applications to the determination of interstellar reddening and stellar populations are discussed.

I. INTRODUCTION

A knowledge of interstellar reddening and extinction at high and intermediate galactic latitudes is essential in many problems. For example, much of our information about stellar evolution comes from fitting main sequences of globular and galactic clusters, corrected for differential line blanketing, to a standard main sequence and comparing the resulting diagrams to evolutionary models. Yet the distances, ages, and metal abundances determined from this method are often sensitively dependent upon the correction for interstellar reddening. Likewise, the distance to the center of the Galaxy is of fundamental importance in the study of galactic structure and dynamics. Probably the most direct determination of this quantity is that due to Baade (1953) who used the apparent magnitude of the frequency maximum of RR Lyrae stars in a "window" near the galactic center. The result, however, is still indecisive because the interstellar absorption assigned to these stars is uncertain. In fact, part of the uncertainty in the absolute magnitudes of the RR Lyrae stars themselves is due to inaccurate values for interstellar absorption.

Most previous determinations of extinction and reddening at high and intermediate galactic latitudes have been derived from galaxy counts and colors of galaxies and clusters because O and B stars, the commonly used reddening indicators, are concentrated in the plane. Late-type stars can be used only if accurate spectral types and luminosity classes are known. Clearly, another class of objects is needed for this purpose.

The RR Lyrae stars are likely candidates. They are easily identified, they have moderately high luminosities, they are found in all parts of the Galaxy, and, as shown in this paper, accurate intrinsic colors can be defined for them.

A number of photoelectric light-curves of Bailey type *a*, *b* RR Lyrae stars based on the *UBV* system are now available. An examination of these curves reveals that the $B - V$ and $U - B$ colors are nearly constant for a large portion of the light cycle preceding minimum light (Preston 1964). It is further noticeable that the stars of this group which are located at high galactic latitudes, where irregularities in color excess are minimal, have nearly uniform colors near minimum light. This indictes that the intrinsic colors of these stars are probably very similar.

Before accurate intrinsic colors can be found for these objects a number of effects

* *Contributions from the Lick Observatory*, No. 191.

† Now at the Department of Physics and Astronomy, University of Rochester.

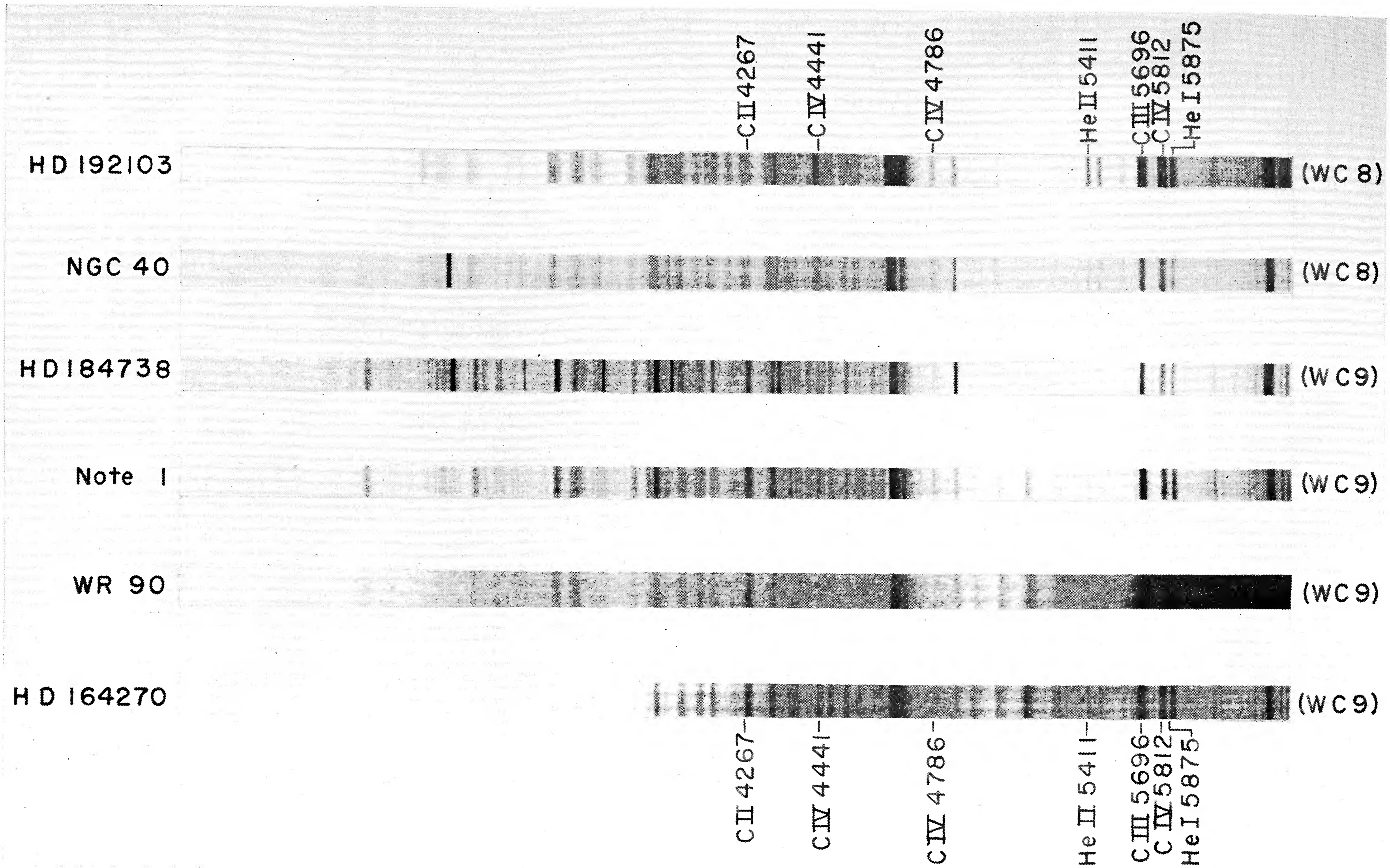

FIG. 4.—Wolf-Rayet carbon stars differing from the sequence illustrated in Fig. 3. Note 1. (1875) $\alpha = 18^{h}31^{m}1$; $-10° + 13'$. HD 184738 is BD+30°3639; Campbell's "hydrogen-envelope star."

must be considered. Preston (1959) has shown that the metal lines in RR Lyrae stars vary greatly in strength. Spinrad (1961) has argued that the weak-lined variables have sizable $B - V$ and $U - B$ excesses compared to the strong-lined variables. The dependence of the colors upon period should also be considered. Finally, the RR Lyrae stars are at such great distances that even those in the galactic caps may be reddened.

The present study is a photometric survey of over 100 field RR Lyrae stars. The next section describes the observational procedure. In § III the effects of line blanketing, period, and interstellar reddening are considered in deriving an intrinsic color relation for these stars. Some applications of the results are discussed in the final section.

II. OBSERVATIONS

The survey was limited to Bailey type *a*, *b* RR Lyrae stars north of $\delta = -15°$ and brighter than $m_v = 14$ at minimum light. Periods were taken from the second edition of the *General Catalogue of Variable Stars*. To avoid type *c* variables, stars with periods less than $0^d.4$ were not observed unless an amplitude of at least 1 mag. was indicated.

Comparison stars, chosen at the telescope, were observed with 95 per cent of the variables. Only a few of the comparison stars lie further than half a degree from the variable, and the average difference between the color of a comparison and variable near minimum light is only 0.13 mag. in $B - V$. The comparison stars are, on the average, 1.3 mag. brighter than the variables and should therefore be more accurately measured.

Primary and secondary *UBV* standards were observed each night and used to transform both the variable and comparison stars to the *UBV* system. An average of all observations of the comparison star was formed and each observation of the variable corrected by the residual of the comparison from this average. The observations from July, 1963, until May, 1964, were reduced with the IBM 7090 computer of the University of California, Berkeley, by a program written by C. Perry. After this time the reductions were carried out on the IBM 1620 of the Lick Observatory with a program written by T. D. Kinman, J. Smak, and the writer.

Observations were made with the Crossley and 24-inch reflectors of the Lick Observatory and the 36-inch telescope of the Kitt Peak National Observatory. Refrigerated 1P21 photomultipliers were used at all the telescopes. The Crossley and Kitt Peak filters have been described by Webb (1964). The Lick 24-inch filters consisted of: *V*, 3.3 mm Corning 3384; *B*, 1 mm BG 12 + 2 mm GG13; *U*, 3.0 mm Corning 9863; red leak, 3.0 mm Corning 9863 + 1 mm RG1.

The probable errors of a single observation of comparison stars in the interval $12.0 < m_V < 12.5$ are

$$\epsilon(V) = \pm 0.015 \text{ mag.}, \quad \epsilon(B - V) = \pm 0.012 \text{ mag.}, \quad \epsilon(U - B) = \pm 0.017 \text{ mag.}$$

Nine comparison stars were observed on at least two nights both at the Crossley ("Cr") and at Kitt Peak ("KP"). Similarly, another nine were in common between the Crossley and the 24-inch ("24"). The colors of these stars as found at each telescope were averaged. The differences, in the sense of the Kitt Peak 36-inch and the Lick 24-inch minus the Crossley, are

$$(B - V)_{KP} - (B - V)_{Cr} = 0.001 \text{ mag.}, \; (U - B)_{KP} - (U - B)_{Cr} = 0.000 \text{ mag.},$$

$$(B - V)_{24} - (B - V)_{Cr} = 0.002 \text{ mag.}, \; (U - B)_{24} - (U - B)_{Cr} = -0.006 \text{ mag.}$$

Table 1 contains all the observations of stars used in the discussion plus other observations that may be of use to observers of variable stars. The light-curves were shifted to make phase 0.0 coincide with maximum light. The uncertainties ($\sim 0^P.05$) in these shifts are unimportant for our purposes. The first column of Table 1 gives the JD (geocentric) of the observation. An "L" or "K" after the JD indicates that the Lick 24-inch or the

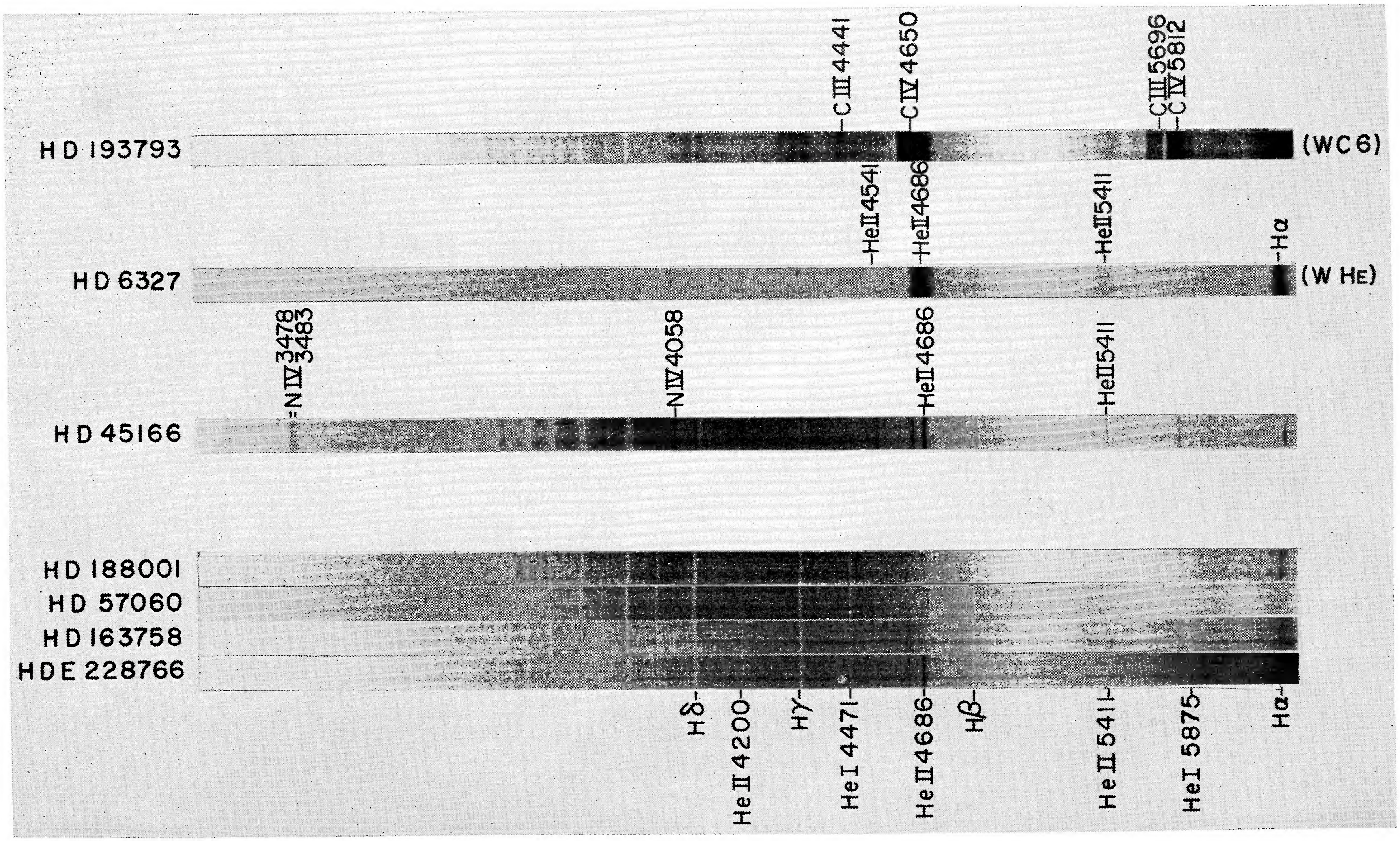

Fig. 5.—Miscellaneous stars. HD 193793 is discussed in the text. HD 6327 seems to be a Wolf-Rayet star without either nitrogen or carbon. HD 45166 is a star often associated with Wolf-Rayet stars. Four Of stars are illustrated for comparison purposes.

1966ApJ...143..774S

TABLE 1

THE OBSERVATIONAL DATA

JD⊕ 2438000+	Phase (Per.)	V	B-V	U-B
SW And		8.932	0.581	0.112
351.710	0.85	10.069	.526	0.153
351.719	.87	10.057	.521	0.165
351.734	.90	9.888	.424	0.097
351.740	.92	9.730	.375	0.068
351.786	.02	9.209	.208	0.173
351.850	.07	9.507	.343	0.193
358.718	.695	9.988	.523*	0.193*
358.759	.79	10.107	.517*	0.187*
364.629	.06	9.307	.242	0.190
364.680	.18	9.531	.353	0.180
364.742	.31	9.725	.451	0.184
364.770	.38	9.813	.484	0.145
397.616	.645	9.953	.531*	0.190*
397.654	.73	10.001	.547*	0.165*
397.679	.785	10.091	.536*	0.166*
397.707	.85	10.116	.533	0.149
XX And		11.126	.490	-0.065
287.834	.68	10.952	.469*	-0.031*
287.845	.695	10.988	.442*	0.006*
288.017	.93	10.668	.246	-0.065
295.928	.88	11.065†	.447†	0.014†
295.988	.96	10.399	.228	0.054
296.000	.98	10.269	.200	0.067
AT And		9.465	.372	0.082
333.620	.245	10.649	.519	0.133
333.631	.26	10.678	.524	0.159
333.655	.30	10.706	.553	0.112
333.690	.36	10.736	.557	0.104
333.718	.40	10.747	.582	0.093
333.740	.44	10.817	.550	0.143
333.784	.51	10.851	.555*	0.085*
333.811	.55	10.835	.592*	0.142*
333.818	.565	10.866	.560*	0.093*
334.643	.90	10.594	.462	0.067
334.667	.94	10.543	.421	0.080
334.688	.97	10.467	.391	0.135
334.703	.00	10.416	.422	0.141
334.723	.03	10.435	.426	0.103
334.738	.055	10.434	.463	0.126
334.768	.105	10.518	.457	0.121
334.786	.135	10.560	.480	0.074
SX Aqr		11.181	.543	-0.042
587.889	.30	11.777	.340	0.064
587.945	.40	11.891	.434	0.032
589.851L	.96	11.528	.193	0.012
589.862L	.98	11.263	.141	0.092
591.852	.70	12.125	.432*	0.013*
592.860	.58	12.144	.447*	0.001*
592.928	.71	12.117	.408*	0.043*
605.816	.76	12.123	.406*	0.017*
612.795L	0.79	12.064	0.405*	-0.011*
SX Aqr (continued)				
621.801L	0.60	12.153	0.408*	0.066*
621.842L	.68	12.126	.416*	0.056*
621.884L	.76	12.092	.404*	0.046*
TZ Aqr		10.398	.523	-0.001
238.956	.08	11.985†	.264†	0.040†
243.957	.84	12.476†	.464*†	0.024*†
263.806	.58	12.344	.467*	0.008*
298.715	.70	12.342	.460*	0.056*
367.631	.35	12.160	.461	0.099
YZ Aqr		10.381	.315	0.002
283.750	.24	12.571	.351	0.066
286.815	.80	12.917	.460*	-0.016*
287.758	.50	12.894	.463*	0.032*
298.745	.41	12.764	.506*	0.114*
326.668	.00	12.095†	.140†	0.077†
BN Aqr		12.328	.556	-0.030
315.756	.00	11.820	.098	0.018
315.772	.03	11.938	.111	0.076
326.654	.20	12.410	.296	0.084
326.700	.30	12.575	.390	0.080
326.741	.39	12.749	.393	0.015
326.750	.41	12.787	.374	-0.001
328.723	.61	12.924	.398*	-0.082*
BR Aqr		11.065	.636	0.144
243.972	.22	11.316	.315	0.055
255.913	.00	10.768	.138	0.101
263.793	.35	11.518	.406	0.084
263.936	.65	11.691	.471*	0.111*
283.773	.81	11.864	.446*	0.077*
376.639	.53	11.674	.415*	0.031*
CP Aqr		11.761	.696	0.212
238.900	.94	11.758	.135	-0.016
240.893	.24	11.677	.340	0.187
298.816	.23	11.686	.286	0.169
298.731	.05	11.193	.140	0.083
283.735	.68	12.098	0.512*	0.112*
AA Aql		9.426	1.302	1.338
243.770	.40	11.985	0.470*	0.128*
243.867	.66	12.181	.464*	0.169*
243.890	.73	12.374†	.447*†	0.102*†
263.862	.935	12.088	.376	0.008
263.869	.955	11.723	.335	0.008
298.666	.14	11.402	.217	0.188
341 Aql		8.853	.224	0.170
263.852	0.90	11.400†	0.476†	0.050†

TABLE 1 (Continued)

JD⊕ 2438000+	Phase (Per.)	V	B-V	U-B
341 Aql (continued)				
276.758	0.225	10.640†	0.241†	0.200†
594.797L	.45	10.985	.441	0.085
594.808L	.47	11.025	.429	0.098
594.859L	.56	11.096	.449*	0.107*
594.902L	.63	11.148	.460*	0.123*
594.945L	.70	11.240	.467*	0.102*†
605.872	.61	11.124	.454*	0.094*
605.925	.70	11.243	.443*	0.070*
618.721	.84	11.292	.452*	0.088*
619.757	.63	11.160	.454*	0.073*
X Ari		7.291	.427	-0.007
364.645	.60	9.805	.579*	0.072*
364.694	.675	9.851	.567*	0.054*
364.761	.775	9.809	.543*	0.031*
364.787	.82	9.866	.546*	0.094*
367.652	.22	9.413	.449	0.134
367.688	.27	9.505	.465	0.116
367.711	.305	9.552	.483	0.069
367.772	.40	9.668	.540	0.087
367.825	.48	9.744	.574*	0.067*
376.627	.00	9.053	.305	0.162
376.711	.065	9.221	.370	0.175
386.704	.48	9.762	.562*	0.068*
386.761	.565	9.820	.566*	0.060*
386.770	.58	9.820	.581*	0.079*
410.612	.195	9.363	.418	0.132
410.670	.285	9.497	.482	0.130
TZ Aur		12.392	.516	-0.014
435.680	.96	11.147	.092	0.022
435.690	.985	11.114	.083	0.008
440.630K	.60	12.253	.437*	0.198*
440.710K	.80	12.404	.502*	0.175*
440.786K	.00	11.085†	.215†	-0.075†
441.643K	.18	11.694†	.324†	0.246†
441.728K	.40	12.134	.470*	0.192*
ST Boo		10.157	.543	-0.085
506.845K	.20	10.913	.262	0.079
506.905K	.30	11.085	.310	0.077
506.965K	.395	11.172	.380	0.037
528.801L	.48	11.200	.431*	-0.021
528.933L	.69	11.297	.418*	0.056*
558.708L	.54	11.220	.411*	0.027*
558.779L	.655	11.281	.405*	0.079*
558.800L	.68	11.292	.406*	0.041*
SV Boo		12.545	.561	0.017
469.906K	.65	13.448	.393*	0.044*
470.001K	.81	13.508	.447*	0.053*
473.865K	.46	13.339	.430*	0.055*
526.834	.56	13.378	.459*	-0.016*
526.950	.76	13.440	.489*	-0.062*
528.900L	0.11	12.883	0.284	-0.108
SW Boo		12.253	0.660	0.211
469.895K	0.30	12.537	.344	0.082
469.991K	.485	12.816	.412*	-0.020*
473.884K	.065	12.032	.148	0.194
493.788	.83	12.928	.345	0.035
498.810	.61	12.739	.427*	0.098*
579.731L	.19	12.261	.300	0.158
579.786L	.30	12.467	.351	0.101
579.795L	.315	12.553	.334	0.109
587.708	.725	12.800	.405*	-0.011*
589.719L	.64	12.801	.397*	0.060*
TW Boo		9.985	.501	0.021
469.915K	.20	11.196	.284	0.112
469.973K	.31	11.373	.351	0.082
473.843K	.58	11.616	.445*	0.032*
473.909K	.705	11.616	.430*	0.032*
473.945K	.77	11.639	.397*	0.067*
505.830K	.675	11.633	.397*	0.054*
505.865K	.74	11.613	.370*	0.049*
505.916K	.83	11.714	.432*	0.036*
UU Boo		11.461	.457	-0.076
493.955	.50	12.666	.396*	0.001*
493.990	.575	12.737	.408*	-0.028*
527.979	.97	12.209	.173	-0.033
527.984	.98	11.970	.159	-0.075
526.820	.43	12.562	.362	0.044
526.891	.585	12.730	.398*	0.047*
526.936	.68	12.743	.367*	0.004*
526.984	.79	12.703	.388*	-0.058*
UY Boo		10.667	.484	-0.019
473.925K	.60	11.259	.388*	0.029*
491.784	.04	10.636	.215	0.067
491.909	.23	10.908	.325	0.036
491.962	.315	11.013	.392	-0.016
492.898	.75	11.248	.394*	-0.033*
492.975	.87	11.244	.435	-0.065
526.727	.73	11.267	.413*	-0.026*
526.786	.825	11.352	.402*	0.006*
RW Cnc		11.493	.628	0.052
386.906	.98	11.287	.118	0.066
386.914	.995	11.248	.130	0.042
387.010	.17	11.654	.260	0.060
409.788	.80	12.154	.395*	0.013*
428.781	.505	12.060	.425*	-0.026*
428.810	.56	12.074	.425*	0.036*
428.823	.58	12.086	.407*	-0.021*
428.863	.655	12.101	.402*	0.009*
SS Cnc		10.977	.444	-0.024
386.895	.54	12.596	.501*	0.190*
386.976	.76	12.749	.501*	0.170*
387.066	0.005	11.764	0.157	0.188

TABLE 1 (Continued)

JD⊕ 2438000+	Phase (Per.)	V	B-V	U-B
SS Cnc (continued)				
351.965	0.45	12.501	0.452	0.285
351.980	.49	12.503	.461	0.226
435.801	.68	12.694	.510*	0.246*
428.833	.81	12.707	.542*	0.190*
TT Cnc		11.383	.179	0.137
351.999	.92	11.371	.419	0.031
432.743	.23	11.242	.375	0.099
432.801	.34	11.383	.452	0.075
432.887	.49	11.572	.484*	0.094*
432.918	.54	11.598	.534*	0.069*
435.850	.73	11.610	.446*	0.114*
492.666	.57	11.578	.494*	0.046*
492.713	.65	11.596	.498*	0.033*
492.777	.76	11.658	.445*	0.075*
W Cvn		9.456	.448	-0.007
469.888K	.90	10.850	.392	-0.005
469.988K	.08	10.180	.215	0.150
473.957K	.275	10.518	.349	0.098
505.699K	.80	10.880	.418*	0.086*
506.680K	.58	10.755	.468*	0.074*
506.731K	.67	10.792†	.435*†	0.054*†
506.764K	.73	10.809	.400*	0.077*
528.756L	.415	10.773	.445	0.059
560.736L	.55	10.785	.421*	0.076*
560.789L	.645	10.820	.430*	0.055*
Z Cvn		12.115	.655	0.146
444.787K	.80	12.191	.390*	0.009*
444.905K	.98	11.574	.127	0.110
445.015K	.15	11.789	.272	0.092
474.735K	.60	12.190	.407*	-0.036*
474.775K	.66	12.206	.405*	0.011*
RR Cvn		12.055	.585	-0.009
443.861K	.20	12.614	.321	0.134
443.978K	.41	12.928	.380	0.053
444.752K	.80	13.112	.410*	0.029*
444.874K	.015	12.161	.168	0.203
469.750K	.545	12.977	.435*	0.068*
473.779K	.76	13.154	.379*	0.123*
493.854	.70	13.030	.413*	0.053*
SW Cvn		12.582	.484	-0.228
441.842K	.40	13.203	.434*	0.059*
443.869K	.99	12.294†	.084†	0.166†
443.956K	.19	12.967	.219	0.208
445.011K	.575	13.332	.412*	0.038*
473.768K	.69	13.367	.386*	0.012*
473.816K	.80	13.444	.382*	0.045*
526.770	.70	13.382	.366*	0.017*
526.800	0.77	13.425	0.321*	0.046*
SZ Cvn		10.390	0.563	0.070
469.880K	0.40	13.113	.372	0.045
469.952K	.53	13.254	.428*	0.023*
470.012K	.64	13.291	.407*	0.030*
473.969K	.84	13.298	.419	0.002
474.763K	.28	12.963	.308	0.072
498.757	.935	12.996	.245	---
RV Cap				
238.888	.03	10.615†	-0.013†	0.068†
240.883	.49	11.276†	0.430*†	0.017*†
283.786	.31	10.952†	.263†	0.059†
RV Cet		11.183	.382	-0.038
287.920	.90	10.843	.326	-0.043
287.929	.915	10.804	.327	-0.017
295.911	.72	11.105	.400*	0.045*
326.824	.31	10.874	.386	0.014
326.913	.45	10.973	.450*	0.048*
409.609	.105	10.630	.273	0.068
RX Cet		11.790	.567	-0.015
283.800	.20	11.208	.331	-0.010
283.821	.24	11.293	.340	-0.004
286.841	.50	11.584	.430*	0.045*
328.811	.655	11.649	.436*	-0.005*
358.697	.75	11.731	.342	0.043†
RZ Cet		9.819	.347	-0.018
286.912	.00	11.244	.122	0.078
298.889	.455	11.949	.412*	0.018*
315.897	.76	12.165	.401*	0.009*
315.946	.86	12.148	.386*	0.006*
326.815	.14	11.486	.230	0.077
326.855	.225	11.639	.268	0.040
326.907	.33	11.789	.334	---
UU Cet		10.456	.536	0.079
287.811	.90	12.136	.433	-0.083
287.822	.92	12.081	.358	-0.084
295.888	.16	11.899	.328	-0.012
295.897	.17	11.910	.332	-0.037
298.837	.09	11.734	.218	0.065
367.613	.57	12.186	.440*	0.053*
367.663	.65	12.207	.404*	-0.015*
S Com		10.167	.289	0.022
428.911	.65	12.009	.403*	-0.001*
428.944	.705	12.051	.392*	0.000*
428.979	.765	11.991	.374*	0.047*
429.005	.81	12.068	.376*	0.032*
432.859	.38	11.801	.360	0.035
432.927	.50	11.941	.383*	0.033*
433.001	0.62	11.977	0.406*	0.017*

TABLE 1 (Continued)

$JD_{\oplus}$ 2438000+	Phase (Per.)	V	B-V	U-B
S Com (continued)				
440.857K	0.015	10.935	0.046	0.107
443.839K	.10	11.173	.116	0.194
443.920K	.24	11.525	.253	0.135
443.947K	.285	11.605	.281	0.114
V Com		11.470	.596	0.072
432.940	.90	13.535†	.384†	-0.046†
432.949	.92	13.292	.224	-0.044
433.020	.07	12.954†	.085†	0.137†
435.941	.29	13.505†	.310†	0.022†
436.037	.50	13.763†	.401*†	0.064*†
444.897K	.38	13.579	.376	0.084
463.791	.66	13.734	.396*	0.046*
463.824	.73	13.770	.384*	0.020*
463.838	.76	13.743	.418*	0.019*
Z Com		12.092	.624	0.003
493.709	.94	13.884	.293	---
493.725	.97	13.476	.150	---
494.700	.75	14.128	.450*	---
494.713	.77	14.135	.469*	---
494.719	.78	14.168	.418*	---
494.730	.80	14.219	.433*	---
494.752	.85	14.238	.443	---
494.761	.86	14.267	.410	---
RY Com		10.331	.624	0.078
492.727	.48	12.661	.410*	0.014*
492.814	.665	12.815	.373*	0.005*
492.923	.90	12.770	.352	-0.013
493.908	.00	12.152	.124	0.033
530.770	.60	12.827	.405*	0.026*
530.827	.72	12.867†	.398*†	0.091*†
UY Cyg		11.241	.311	0.163
577.911	.73	11.377	.510*	0.089*
577.975	.85	11.428	.476	0.164
579.827L	.15	10.756	.241	0.207
579.947L	.36	11.061	.446	0.110
586.907	.77	11.370	.455*	0.111*
591.813	.52	11.237	.533*	0.136*
605.888	.63	11.318	.496*	0.116*
605.946	.73	11.384	.500*	0.085*
618.775	.61	11.387	.464*	0.119*
618.843	.73	11.401	.475*	0.119*
619.856	.54	11.313	.468*	0.117*
622.717L	.64	11.324	.516*	0.120*
622.727L	.66	11.365	.483*	0.114*
622.745L	.69	11.321	.515*	0.091*
622.781L	.76	11.350	.489*	0.080*
XZ Cyg		10.912	.214	0.189
594.704L	.35	9.865	.367	0.099
594.713L	0.37	9.879	0.384	0.094
XZ Cyg (continued)				
594.748L	0.44	9.998	0.394*	0.064*
594.785L	.53	10.090	.415*	0.052*
594.820L	.60	10.112	.424*	0.056*
594.844L	.65	10.110	.392*	0.061*
594.882L	.73	10.079	.395*	0.059*
594.922L	.81	10.160	.391*	0.078*
594.972L	.93	9.492	.208	0.032
612.772L	.075	9.368	.211	0.201
621.674L	.15	9.579	.266	0.160
621.682L	.17	9.610	.276	0.145
621.829L	.485	9.951	.416*	0.066*
621.872L	.58	10.031	.399*	0.087*
622.818L	.605	10.036	.411*	0.060*
DM Cyg		12.551	.550	0.010
230.942	.95	11.962†	.604†	---
231.951	.36	11.586†	.523†	0.236†
255.972	.55	11.739†	.622†	0.217†
326.709	.05	10.965†	.246†	0.196†
326.772	.20	11.296†	.374†	0.203†
586.937	.85	11.988	.585*	0.237*
586.968	.92	11.886	.512	0.181
587.959	.285	11.468	.449	0.231
593.893L	.42	11.604	.513	0.295
619.925	.42	11.605	.522	0.271
622.900L	.505	11.722	.531*	0.227*
RW Dra		9.548	.598	0.077
505.961K	.47	12.009	.398*	0.073*
528.959L	.40	11.836	.357	0.066
589.708L	.56	12.041	.413*	0.108*
589.765L	.69	12.077	.418*	0.053*
589.813L	.80	12.063	.391*	0.065*
593.743L	.67	12.056	.412*	0.014*
XZ Dra		10.493	.572	0.041
568.753L	.35	10.317	.413	0.157
568.827L	.51	10.462	.456*	0.107*
568.894L	.65	10.551	.469*	0.146*
579.838L	.62	10.587	.474*	0.145*
579.897L	.74	10.630	.461*	0.129*
AE Dra		10.154	.536	-0.043
560.926L	.15	12.421	.290	0.135
560.964L	.21	12.513	.371	0.109
579.850L	.55	12.874	.412*	0.074*
579.909L	.65	12.853	.431*	0.078*
593.731L	.58	12.789	.475*	-0.022
593.776L	.66	12.823	.446*	0.113*
593.828L	.74	12.894	.483*	0.172
RX Eri		8.277	.493	0.003
386.740	.02	9.276	.246	0.125
386.818	0.15	9.545	0.328	0.078

TABLE 1 (Continued)

JD⊕ 2438000+	Phase (Per.)	V	B-V	U-B
RX Eri (continued)				
386.863	0.23	9.658	0.390	0.083
410.648	.73	10.007	.472*	0.025*
431.683	.55	9.896	.510*	0.066*
440.645K	.81	10.071	.480*	0.088*
441.650K	.52	9.859†	.477*†	0.098*†
444.633K	.60	9.929	.467*	0.097*
SV Eri		11.325	.523	0.047
315.865	.935	9.631	.303	0.087
315.874	.95	9.661	.278	0.104
315.925	.02	9.559	.267	0.087
326.786	.24	9.900	.320	0.046
326.836	.31	9.959	.377	0.065
326.924	.43	10.083	.437	-0.002
410.634	.71	10.231	.452*	-0.013*
410.659	.745	10.201	.435*	-0.011*
UZ Eri		9.838	.424	-0.058
298.947	.97	12.408	.193	0.086
315.939	.17	12.632	.299	0.058
326.885	.045	12.337	.197	0.083
326.942	.13	12.565	.244	0.103
351.748	.37	12.978	.445	0.020
351.804	.46	13.266	.400	-0.009
351.817	.48	13.199	.435	-0.009
409.623	.60	13.153	.481*	-0.001*
409.633	.62	13.163	.480*	0.024*
409.704	.73	13.181	.453*	0.010*
BB Eri		13.051	.462	-0.066
426.708	.65	11.741	.408*	---
426.723	.675	11.700	.423*	---
431.618	.26	11.433	.332	0.016
431.654	.33	11.578	.366	0.039
432.620	.02	11.066	.115	0.051
432.729	.215	11.422	.317	0.038
435.718	.46	11.655	.405*	0.039*
441.605K	.79	11.773	.415*	0.052*
441.659K	.88	11.762	.398	-0.018
443.654K	.38	11.597	.406	0.031
BK Eri		8.138	.507	-0.105
286.934	.95	12.214	.212	-0.005
286.941	.965	12.095	.174	-0.038
287.004	.15	12.200	.184	0.186
261.010	.16	12.237	.198	0.180
298.904	.765	12.962	.405*	-0.086*
326.800	.565	12.931	.395*	-0.026*
328.844	.34	12.837	.443	-0.044
RR Gem		10.273	.370	-0.024
327.020	.20	11.353	.399	0.191
426.753	0.25	11.410	0.427	0.207

JD⊕ 2438000+	Phase (Per.)	V	B-V	U-B
RR Gem (continued)				
426.763	0.27	11.446	0.444	0.215
426.788	.335	11.536	.476	0.208
426.797	.36	11.550	.495	0.200
426.811	.40	11.576	.472	0.162
426.832	.45	11.592	.498	0.187
426.843	.475	11.615	.507	0.202
426.854	.50	11.682	.495*	0.196*
426.864	.53	11.701	.501*	0.210*
426.874	.555	11.687	.521*	0.196*
426.883	.575	11.698	.515*	0.205*
431.668	.63	11.691	.546*	0.133*
431.709	.74	11.815	.525*	0.238*
431.720	.77	11.805	.567*	0.177*
431.752	.84	11.806	.490	0.137
431.811	.98	10.743	.146	0.177
AK Gem		14.066	.339	0.166
432.650	.60	13.842	.587*	0.176
432.714	.72	13.976	.534*	0.290
432.778	.84	14.130	.573*	0.072
432.874	.025	13.326	.275†	0.195†
435.659	.29	13.480	.348	-0.010
435.732	.425	13.814	.543	0.283
GI Gem				
351.934	.61	13.253†	.449*†	0.137*†
351.955	.66	13.333†	.441*†	0.016*†
409.748	.05	12.389†	.182†	0.138†
409.756	.07	12.459†	.194†	0.173†
431.740	.81	13.458†	.482*†	0.093*†
431.784	.91	13.351†	.561†	0.037†
428.764	.94	13.099†	.309†	0.039†
428.766	.945	12.948†	.335†	-0.023†
428.774	.96	12.732†	.210†	0.061†
441.615K	.60	13.298†	.470*†	0.211*†
441.693K	.78	13.354†	.541*†	0.142*†
441.748K	.91	13.390†	.475†	0.156†
444.695K	.80	13.402†	.421*†	0.224*†
TW Her		10.554	.266	-0.004
240.719	.36	11.548	.426	0.142
243.718	.86	10.570	.105	0.091
275.747	.015	10.942	.197	0.192
275.757	.04	10.993	.248	0.178
275.796	.14	11.195	.341	0.127
275.802	.15	11.233	.369	---
558.909L	.62	11.687	.445*	0.179*
558.948L	.725	11.812	.460*	0.221*
577.747	.77	11.824	.439*	0.084
577.827	.97	10.801	.188	0.200
591.704	.70	11.790	.481*	0.151*
592.826	.505	11.628	.470*	0.164*
VX Her		10.711	0.584	0.044

TABLE 1 (Continued)

JD⊕ 2438000+	Phase (Per.)	V	B-V	U-B
VX Her (continued)				
230.800	0.025	9.937†	0.113†	0.105†
231.752	.115	10.314†	.180†	0.160†
234.713	.62	11.108	.465	0.007
238.718	.41	10.817	.393	0.093
255.797	.92	10.948	.372	0.021
263.721	.32	10.793	.382	0.047
568.722L	.105	10.315	.199	0.218
568.734L	.13	10.404	.225	0.212
568.800L	.28	10.740	.325	0.147
568.877L	.445	11.025	.406	0.060
575.749L	.54	11.111†	.443*†	0.066*†
575.778L	.60	11.163	.418*	0.090*
575.809L	.67	11.085†	.438*†	0.066*†
575.847L	.75	11.115	.408*	0.077*
579.705L	.225	10.650	.309	0.171
591.745	.665	11.116	.434*	0.071*
VZ Her		10.947	.510	0.050
547.756L	.40	11.753	.351	0.092†
577.767	.555	11.887	.433*	0.066*
577.818	.67	11.891	.399*	0.079*
577.860	.77	11.910	.381*	0.040*
577.892	.84	12.035	.360	0.017
577.931	.93	11.311	---	---
577.934	.94	11.171	.136	0.050
577.942	.95	10.843	.065	0.075
577.945	.96	10.753	.073	0.065
577.949	.97	10.716	.059	0.056
582.741	.85	12.007	.404	0.077
582.772	.92	11.474	.238	-0.031
592.703	.48	11.861	.420*	0.071*
592.765	.62	11.901	.417*	0.053*
592.808	.71	11.919	.416*	0.032*
592.842	.79	11.908	.414*	0.073*
AR Her		9.886	.498	-0.001
506.884K	.90	11.294	.284	-0.019
506.929K	.995	10.592	.074	0.074
528.829L	.59	11.553	.382*	0.009*
528.879L	.70	11.600	.333*	0.009*
528.924L	.79	11.524	.327*	0.010*
526.907	.50	11.534	.350*	0.006*
560.777L	.56	11.504	.375*	0.042*
560.814L	.64	11.570	.350*	0.067*
BD Her		11.391	.539	0.114
585.918	.90	12.547	.593	0.131
585.934	.935	12.180	.432	0.195
585.938	.945	12.089	.435	0.187
586.731	.61	12.584	.654*	0.197*
586.802	.76	12.692	.612*	0.259*
592.879	.59	12.539	.643*	0.272*
612.761L	.54	12.451	.614*	0.259*
621.765L	0.54	12.457	0.609*	0.325*

JD⊕ 2438000+	Phase (Per.)	V	B-V	U-B
CE Her				
231.765	0.25	12.302†	0.393†	0.120†
238.734	.01	11.658†	.155†	0.173†
287.697	.51	12.689†	.513*†	0.023*†
298.642	.55	12.688†	.500*†	0.079*†
326.613	.68	12.722†	.488*†	-0.010*†
EE Her		11.405	.653	0.146
527.936	.75	13.549†	.489*†	0.111*†
527.952	.78	13.619	.463*	0.101*
530.811	.55	13.462	.453*	0.121*
587.802	.56	13.430	.485*	0.103*
EP Her		11.044	.483	-0.036
585.802	.95	13.189	---	---
585.812	.97	12.751	.152	0.067
585.818	.99	12.438	.115	0.097
587.765	.56	13.542	.493*	0.065*
587.816	.68	13.537	.432*	0.046*
593.790L	.71	13.449	.486*	0.149*
619.695	.56	13.537	.475*	0.072*
619.725	.63	13.534	.461*	0.090*
619.777	.755	13.544	.445*	0.113
OS Her		10.799	.676	0.186
585.851	.02	13.256	.121	0.186
585.861	.055	13.346	.143	0.177
585.895	.13	13.623	.230	0.215
586.840	.51	14.270	.443*	0.057
586.887	.64	14.235	.471*	---
587.736	.775	14.356	.474*	0.173*
619.711	.49	14.219	.392	0.181*
619.745	.58	14.223	.470*	0.171*
619.806	.73	14.307	.522*	0.173*
OX Her		9.920	.759	0.224
580.757	.90	13.172	.441	0.025
580.804	.96	12.875	.372	0.036
582.821	.625	13.252	.453*	-0.003*
582.897	.725	13.287	.434*	0.021*
582.947	.79	13.351	.433*	0.023*
RR Leo		10.400	.090	0.105
440.698K	.80	11.125	.422*	0.062*
440.738K	.89	11.248	.392	0.104
441.704K	.02	9.949	.113	0.150
441.795K	.22	10.620	.252	0.159
441.891K	.435	10.976†	.413†	0.099†
444.688K	.62	11.125	.406*	0.104*
RX Leo		11.792	.425	-0.041
443.766K	.15	11.727	.309	0.098
443.877K	.32	11.895	.418	0.103
444.007K	0.52	12.092	0.449*	0.060*

TABLE 1 (Continued)

JD⊕ 2438000+	Phase (Per.)	V	B-V	U-B
RX Leo (continued)				
444.796K	0.725	12.178	0.458*	0.054*
444.918K	.91	12.002	.351	0.047
489.815	.625	12.094	.461*	0.033*
489.860	.69	12.149	.448*	0.076*
491.730	.55	12.094	.438*	0.067*
491.865	.76	12.212	.475*	0.031*
SS Leo				
449.811	.91	11.356†	.359†	-0.037†
449.870	.00	10.413†	.098†	0.096†
449.963	.14	10.813†	.219†	0.107†
463.847	.315	11.111†	.331†	0.034†
474.693K	.725	11.380†	.397*†	0.012*†
474.719K	.77	11.464†	.403*†	-0.021*†
474.785K	.87	11.511†	.396†	0.005†
492.695	.37	11.160†	.386†	0.039†
506.651K	.75	11.364†	.427*†	0.054*†
506.711K	.78	11.403†	.386*†	0.050*†
ST Leo		11.290	.473	-0.064
469.736K	.78	11.926	.368*	0.117*
469.842K	.00	10.772	.081	0.130
469.929K	.18	11.296	.269	0.176
474.753K	.275	11.481	.368	0.116
473.854K	.395	11.739	.387	0.118
473.899K	.49	11.833	.441*	0.092*
489.791	.74	11.907	.411*	0.055*
491.713	.76	11.914	.393*	0.044*
SU Leo		12.817	.527	-0.005
386.938	.50	13.835	.399*	0.050*
435.750	.86	13.948	.404*	-0.021*
435.836	.04	12.805	.024	0.054
435.912	.20	13.254	.190	0.130
435.991	.365	13.633	.305	0.114
441.785K	.64	13.942	.429*	0.098*
441.882K	.85	13.988	.378*	-0.008*
WW Leo		12.202	.504	-0.051
386.925	.32	12.593	.472	0.057
428.881	.94	12.348	.292	0.029
432.845	.52	12.739	.498*	0.068*
432.988	.75	12.840	.481*	0.034*
469.625K	.55	12.765	.472*	0.063*
469.650K	.59	12.816	.396*	0.125*
AA Leo		11.299	.476	-0.057
443.900K	.40	12.520	.426	0.092
443.968K	.515	12.624	.430*	0.046*
444.737K	.80	12.869	.426*	0.096*
444.855K	.00	11.734	.139	0.154
444.967K	.18	12.259	.305	0.071
491.758	.34	12.483	.404	0.042
526.688	.69	12.688	.436*	0.013*
526.709	0.725	12.715	0.449*	0.052*

JD⊕ 2438000+	Phase (Per.)	V	B-V	U-B
V Lmi		10.533	0.439	-0.070
440.729K	0.95	11.517	.211	0.010
440.841K	.16	11.538	.191	0.162
441.718K	.77	12.118	.416*†	0.056*†
444.717K	.28	11.750	.309	0.123
444.833K	.495	12.069	.382*	0.055*
469.698K	.21	11.646	.248	0.135
469.804K	.405	11.938	.394	0.082
474.629K	.275	11.749	.274	0.146
474.638K	.29	11.776	.319	0.098
474.661K	.33	11.866	.364	0.076
473.688K	.545	12.095	.395*	0.050*
473.709K	.585	12.085	.412*	0.054*
473.721K	.605	12.096	.420*	0.040*
Y Lmi		12.332	.570	0.044
440.720K	.115	12.490	.255	0.135
440.827K	.315	12.896	.420	0.042
444.761K	.86	13.015	.332	0.006
443.699K	.795	13.069	.401*	-0.020*
469.659K	.29	12.809	.376	0.081
469.708K	.40	12.951	.393	0.016
469.761K	.49	13.007	.441*	0.054*
469.795K	.55	13.068	.430*	-0.025*
489.828	.75	12.997	.347*	-0.067*
TT Lyn		10.933	.319	0.019
440.689K	.08	9.517	.247	0.128
440.747K	.18	9.670	.310	0.107
441.680K	.74	10.051	.415*	0.005*
441.743K	.84	10.165	.427	0.071
443.797K	.28	9.779	.369	0.115
443.850K	.37	9.894	.432	0.088
463.722	.635	10.061	.435*	0.035*
463.734	.655	10.062	.439*	0.025*
463.749	.68	10.047	.432*	0.032*
463.759	.70	10.044	.435*	0.036*
469.615K	.50	10.023	.448*	0.035*
469.640K	.54	10.029	.468*	0.030*
RZ Lyr		9.800	.166	0.160
587.904	.10	11.471	.307	0.158
587.911	.115	11.519	.320	0.154
587.970	.23	11.559	.365	0.176
589.741L	.69	12.016	.451*	0.034*
589.868L	.94	11.366	.223	0.161
592.745	.57	11.968	.443*	0.084*
592.791	.66	12.032	.446*	0.055*
592.849	.77	12.008	.424*	0.034*
593.839L	.72	11.971	.440*	0.091*
594.725L	.44	11.875	.470*	0.051*
AQ Lyr				
231.845	.92	13.315†	.428†	0.197†
231.875	.00	12.486†	.247†	0.176†
238.845	.52	13.250†	.560*†	0.172*†
238.872	0.59	13.219†	0.548*†	0.249*†

TABLE 1 (Continued)

JD⊕ 2438000+	Phase (Per.)	V	B-V	U-B
AQ Lyr (continued)				
255.742	0.83	13.514†	0.560*†	0.237*†
263.739	.22	12.879†	.415†	0.256†
263.825	.45	13.216†	.574*†	0.253*†
CX Lyr		10.595	.468	-0.046
240.818	.46	13.074	.579	0.153
243.785	.275	12.714	.427	0.278
255.781	.73	13.127†	.564†	0.043†
283.699	.00	12.145	.329	0.246
283.705	.01	12.204	.355	0.268
582.802	.03	12.248	.309	0.257
582.914	.21	12.728	.441	0.251
582.966	.295	12.895	.507	0.191
586.774	.47	13.077	.571	0.148
586.873	.63	13.171	.569*	0.127*
591.796	.615	13.162	.594*	0.145*
IO Lyr		11.296	.482	-0.039
558.927L	.30	11.826	.433	0.146
558.967L	.37	11.937	.424	0.134
560.800L	.55	12.041	.464*	0.124*
560.893L	.71	12.092	.470*	0.080*
560.952L	.81	12.225	.458*	0.102*
KX Lyr		7.260	.502	-0.055
560.940L	.37	11.111	.406	0.201
568.740L	.06	10.489	.157	0.245
568.813L	.22	10.907	.315	0.266
568.887L	.39	11.102	.465	0.209
568.909L	.44	11.197	.435	0.194
593.701L	.67	11.368	.514*	0.169*
612.695L	.75	11.422	.475*	0.155*
612.729L	.83	11.466	.466*	0.142*
621.710L	.195	10.793	.269	0.280
622.756L	.57	11.321	.475*	0.153*
622.794L	.66	11.368	.478*	0.161*
622.837L	.75	11.429	.480*	0.175*
ST Oph		9.579	.525	0.112
231.778	.41	12.350†	.593†	0.232†
234.747	.005	11.338†	.271†	0.302†
238.778	.955	12.127†	.555†	0.151†
255.813	.78	12.513†	.683†	0.302†
263.699	.29	12.142†	.509†	0.246†
579.718L	.00	11.328	.287	0.225
579.770L	.115	11.673†	.402†	0.351†
579.861L	.32	12.169	.574	0.263
582.748	.73	12.557	.615*	0.184*
582.778	.795	12.543	.608*	0.168*
586.718	.54	12.532	.650*	0.168*
586.788	.70	12.514	.609*	0.227*
587.728	.785	12.535	.606*	0.209*
445 Oph		11.377	0.786	0.201

JD⊕ 2438000+	Phase (Per.)	V	B-V	U-B
445 Oph (continued)				
575.716L	0.30	11.030	0.612	0.377
575.731L	.335	11.017	.645	0.418
575.761L	.41	11.088	.700	0.424
575.799L	.51	11.183	.739*	0.465*
575.831L	.59	11.242	.731*	0.445*
587.747	.60	11.236	.706*	0.375*
587.795	.72	11.315	.760*	0.382*
592.712	.11	10.658	.472	0.368
593.714L	.63	11.253	.735*	0.370*
452 Oph		11.958	.684	0.145
231.730	.185	12.023†	.409†	0.218†
240.774	.42	12.333†	.580†	0.128†
276.730	.95	12.559†	.579†	-0.041†
286.708	.86	12.525†	.612†	0.088†
579.756L	.82	12.480	.595*	0.205*†
579.872L	.02	11.685	.297	0.308
580.700L	.51	12.421	.608*	0.201*
580.769L	.64	12.456	.662*	0.178*
585.727	.535	12.504	.603*	0.202*
589.730L	.72	12.504	.651*	0.168*
591.826	.48	12.472	.601*	0.204*
CM Ori		12.311	.493	-0.032
326.970	.00	12.134	.368	0.294
326.980	.015	12.151	.365	0.355
375.832	.50	12.862	.623*	0.171*
409.728	.175	12.494	.527	0.222
431.641	.585	13.002	.657*	0.145*
431.726	.71	13.012	.677*	0.211*
431.797	.82	13.167	.686*	0.136*
VV Peg		12.271	.666	0.113
240.975	.28	11.997†	.420†	-0.016†
255.982	.01	11.496†	.153†	0.165†
294.794	.48	12.237	.411*	-0.007*
294.810	.515	12.243	.427*	0.007*
298.783	.65	12.213	.417*	-0.045*
298.862	.81	12.142	.415*	-0.009*
589.926L	.79	12.279	.421*	-0.008*
592.959	.00	11.413	.160	0.184
605.902	.505	12.243	.447*	0.064*
AE Peg		11.398	.696	0.275
240.965	.80	13.078	.414*	0.049*
243.833	.57	13.101	.468*	-0.079
263.953	.08	12.368	.259	0.162
286.897	.27	12.808	.435	0.023
315.791	.43	13.076	.438*	0.007*
AO Peg		10.271	.392	0.032
286.675	.40	13.073	.503	0.053
286.829	0.68	13.142	0.471*	0.030*

TABLE 1 (Continued)

JD⊕ 2438000+	Phase (Per.)	V	B-V	U-B
AO Peg (continued)				
287.679	0.23	12.897	0.392	0.124
298.800	.56	13.139	.508*	0.071*
376.664	.84	13.348	.449*	0.119*
AV Peg		9.345	.653	0.120
605.795	.10	10.173	.311	0.240
605.805	.125	10.256	.315	0.233
605.957	.515	10.724	.484*	0.176*
618.868	.59	10.789†	.509*†	0.212*†
619.786	.94	9.975	.186	0.152
619.795	.96	9.875	.187	0.184
622.736L	.495	10.688	.505*	0.232*
622.772L	.585	10.744	.521*	0.241*
622.809L	.68	10.801	.532*	0.253*
622.845L	.775	10.906	.539*	0.224*
BF Peg		12.024	.555	0.074
287.725	.00	12.348	.226	0.114
287.740	.03	12.330	.279	0.130
287.863	.28	12.822	.397	0.108
294.739	.145	12.635	.293	0.106
294.752	.17	12.689	.329	0.087
294.821	.31	12.904	.432	0.060
294.829	.325	12.941	.401	0.095
315.800	.625	13.074	.440*	0.077*
315.884	.69	12.990	.428*	-0.025*
CG Peg		11.086	.489	0.043
231.916	.59	11.385†	.542†	0.235†
240.913	.85	11.557†	.576†	0.129†
243.947	.34	11.214†	.467†	0.192†
589.888L	.895	11.468	.497	0.133
589.900L	.92	11.269	.429	0.068
593.913L	.51	11.314	.546*	0.189*
593.955L	.60	11.447	.502*	0.212*
594.955L	.74	11.452	.531*	0.190*
618.763L	.71	11.433	.545*	0.195*
622.863L	.48	11.300	.526*	0.199*
622.888L	.54	11.339	.547*	0.196*
622.912L	.59	11.360	.543*	0.157*
DZ Peg		11.446	.457	-0.019
287.714	.73	12.277	.437*	0.060*
287.872	.99	11.304	.113	0.089
287.904	.04	11.422	.112	0.117
326.641	.82	12.429	.453*	0.021*
328.763	.32	11.989	.365	0.101
351.663	.02	11.311	.108	0.101
351.672	.04	11.344	.126	0.095
AR Per		8.691	.515	-0.013
364.713	.27	10.414	.692	0.307
409.669	0.91	10.591	0.668	0.272

JD⊕ 2438000+	Phase (Per.)	V	B-V	U-B
AR Per (continued)				
409.671	0.915	10.525	0.670	0.265
409.679	.935	10.309	.586	0.245
367.752	.41	10.576	.738	0.372
367.797	.515	10.645	.781*	0.303*
440.606K	.61	10.671	.758*	0.392*
440.666K	.75	10.802	.770*	0.395*
443.677K	.82	10.847	.789*	0.354*
334.825	.03	9.953	.484	0.342
334.834	.05	10.014	.498	0.356
334.861	.11	10.172	.547	0.359
334.870	.14	10.219	.559	0.357
334.885	.17	10.281	.615	0.348
334.900	.21	10.316	.666	0.327
334.910	.23	10.353	.688	0.339
334.919	.25	10.422	.661	0.368
RY Psc		10.734	.713	0.070
328.779	.83	12.641	.448*	-0.003
328.869	.00	12.024	.233	0.280
286.865	.71	12.551	.464*	0.125
287.777	.43	12.507	.408	0.242
298.827	.29	12.444	.375	-0.132
VY Ser		8.442	.505	0.043
488.933	.85	10.522	.430*	0.002*
488.980	.915	10.462	.432	-0.010
489.898	.20	9.954	.326	0.058
491.952	.08	9.747	.251	0.089
492.938	.46	10.221	.449*	0.039*
505.907K	.62	10.358	.422*	0.063*
505.939K	.665	10.346	.450*	0.033*
AN Ser		10.682	.637	0.187
		11.348	.465	0.032
489.913	.12	10.706	.341	0.199
489.997	.28	10.953	.457	0.143
491.941	.005	10.496	.212	0.237
493.920	.795	11.440	.534*	0.268*
505.820K	.59	11.298	.508*	0.296*
527.782	.655	11.348	.568*	0.251*
527.814	.72	11.398	.554*	0.270*
AT Ser		10.003	.477	-0.095
530.917	.09	11.095	.200	0.070
530.931	.11	11.123	.223	0.089
547.715L	.59	11.685	.451*	0.046*
558.885L	.55	11.684	.434*	0.051*
577.703	.76	11.738	.443*	0.072*
577.734	.80	11.873	.422*	0.032*
AV Ser		11.656	.646	0.120
530.886	.15	11.246	.343	0.218
530.898	0.175	11.307	0.376	0.195

TABLE 1 (Continued)

JD⊕ 2438000+	Phase (Per.)	V	B-V	U-B
AV Ser (continued)				
558.849L	0.50	11.761	0.531*	0.218*
558.859L	.52	11.822	.516*	0.214*
560.754L	.41	11.640	.505*	0.226*
560.877L	.66	11.852	.532*	0.167*
AW Ser		11.957	.447	-0.109
527.904	.02	12.386	.178	0.117
527.918	.045	12.480	.178	0.130
530.791	.855	12.998	.319	-0.027
577.722	.45	13.150	.417*	0.021*
577.792	.57	13.205	.435*	0.025*
589.754L	.60	13.213	.461*	0.046*
CS Ser		12.309	.512	-0.064
491.991	.85	12.791	.420	-0.057
493.891	.455	12.715	.489	0.017
493.975	.61	12.811	.392*	0.038*
505.803K	.06	12.131	.183	0.088
505.890K	.22	12.433	.365	0.077
505.975K	.385	12.683	.400	0.039
527.756	.715	12.717	.422*	0.067*
527.795	.79	12.738	.352	-0.041
547.732L	.62	12.682	.441*	0.002*
558.832L	.685	12.718	.389*	0.017*
SS Tau		11.486	.576	0.044
375.783	.76	12.977	.682*	0.320*
375.812	.84	12.986	.668	0.266
375.841	.92	12.757	.498	0.264
375.843	.925	12.703	.459	0.174
375.851	.945	12.337	.382	0.270
376.673	.17	12.308	.520	0.338
376.725	.31	12.680	.542	0.332
376.744	.36	12.740	.602	0.397
376.772	.44	12.795	.597	0.332
386.683	.22	12.522	.518	0.336
386.693	.25	12.570	.538	0.343
386.713	.30	12.699	.570	0.256
386.746	.395	12.787	.604	0.270
386.804	.55	12.949	.681*	0.228*
U Tri				
286.780	.70	12.966†	.445*†	0.158*†
286.803	.75	13.042†	.482*†	0.199*†
286.959	.10	12.187†	.123†	0.177†
287.789	.95	12.816†	.356†	0.055†
287.791	.96	12.718†	.383†	0.085†
287.800	.98	12.516†	.237†	0.063†
287.802	.99	12.418†	.226†	-0.008†
287.972	.55	12.756†	.419*†	0.153*†
386.793	.315	12.718†	.376†	0.161†
RV Uma		10.301	.675	0.173
506.757K	.00	10.371	.148	0.150
506.819K	0.13	10.621	0.260	0.121

JD⊕ 2438000+	Phase (Per.)	V	B-V	U-B
RV Uma (continued)				
506.864K	0.23	10.765	0.311	0.078
506.896K	.295	10.830	.342	0.064
506.935K	.38	10.946	.373	0.061
TU Uma		8.941	.558	0.067
449.761	.56	10.112	.412*	0.010*
449.771	.58	10.098	.426*	0.043*
449.794	.62	10.103	.409*	-0.004*
449.844	.71	10.145	.413*	0.028*
449.897	.805	10.208	.412*	0.000*
450.006	.00	9.388	.222	0.077
469.671K	.26	9.904	.365	0.066
469.730K	.37	10.011	.422†	0.072†
474.650K	.19	9.796	.326	0.069
474.670K	.23	9.835	.360	0.064
474.708K	.30	9.920	.399	0.059
UU Vir		11.604	.531	0.038
449.831	.23	10.706	.361	0.120
449.881	.34	10.838	.395	0.112
449.986	.55	10.923	.410*	0.095*
491.897	.68	11.022	.389*	---
505.667	.63	10.938	.410*	0.088*
505.736K	.775	10.972	.427	0.046*
505.841K	.00	10.249	.194	0.169
UV Vir		11.756	.419	-0.022
435.929	.32	11.884	.377	0.099
436.006	.45	12.066	.406	0.076
441.870K	.44	12.081	.369	0.098
443.887K	.875	12.261	.388	0.076
435.988K	.05	11.350	.109	0.145
444.949K	.685	12.240	.427*	0.072*
473.790K	.81	12.354	.387*	0.087*
491.881	.63	12.203†	.384*†	0.044*†
493.736	.785	12.284	.426*	0.058*
527.691	.62	12.186	.435*	0.070*
AS Vir		11.684	.404	-0.021
435.955	.935	11.813	.265	0.023
436.019	.05	11.618	.203	0.088
488.891	.59	12.120	.432*	---
491.800	.845	12.222	.398	0.025
492.827	.70	12.186	.388*	0.057*
528.710L	.65	12.159	.426*	0.060*
528.770L	.76	12.148	.440*	0.027*
AT Vir		11.675	.452	-0.056
492.765	.30	11.427	.361	0.027
492.838	.44	11.686	.373	0.073
492.909	.575	11.730	.438*	-0.006*
505.677K	.86	11.775	.407*	0.057*
505.745K	.985	10.725	.101	0.112
506.691K	.785	11.715	.346*	0.077*
506.722K	0.845	11.819	0.380*	0.034*

TABLE 1 (Continued)

JD⊕ 2438000+	Phase (Per.)	V	B-V	U-B
AT Vir (continued)				
528.743L	0.725	11.673	0.372*	0.026*
530.752	.545	11.732	.444*	0.002*
BC Vir		11.708	.525	-0.004
527.714	.10	12.019	.227	0.078
527.770	.20	12.190	.340	0.029
547.705L	.51	12.460	.403*	0.109*
560.713L	.56	12.487	.434*	0.067*
BN Vul		10.579	.553	0.072
230.879	.92	10.875†	.864†	---
231.820	.50	11.228†	.862†	0.301†
234.843	.59	11.252†	.899†	0.294†
238.816	.28	10.960†	.834†	0.288†
276.741	0.11	10.627†	0.679†	0.388†
BN Vul (continued)				
276.750	0.125	10.711†	0.698†	0.265†
577.840	.90	11.364	.809	0.301
577.852	.92	11.163	.758	0.263
575.874L	.59	11.249†	.842*†	0.337*†
579.929L	.415	11.119†	.924†	0.391†
579.957L	.46	11.185	.824	0.330
591.840	.46	11.179	.859	0.364
612.718	.605	11.257	.852*	0.314*
612.811L	.76	11.300	.830*	0.330*
618.684	.645	11.288	.869*	0.326*
618.735	.73	11.303	.827*	0.338*
621.722L	.76	11.298	.839*	0.338*
621.754L	.81	11.361	.856*	0.362*
621.782L	.86	11.397	.850	0.347
622.763L	0.51	11.220	0.855*	0.311*

Kitt Peak 36-inch telescope was used. All other observations were obtained at the Crossley. The second column gives the approximate phase. The next three columns give V, $B - V$, and $U - B$ corrected from the comparison star unless otherwise indicated. The first entries for each star are the magnitude and colors of the comparison star used. A dagger ("†") after an observation indicates that a comparison star was not observed. An asterisk ("*") indicates that the observation is used to form the average color index at minimum as described in the next section.

III. ANALYSIS OF THE DATA

a) Color-Index Variations near Minimum Light

The behavior of the $B - V$ and $U - B$ color indices of type *a*, *b* RR Lyrae stars is indicated in Figure 1. The average $B - V$ and $U - B$ color indices for each star were

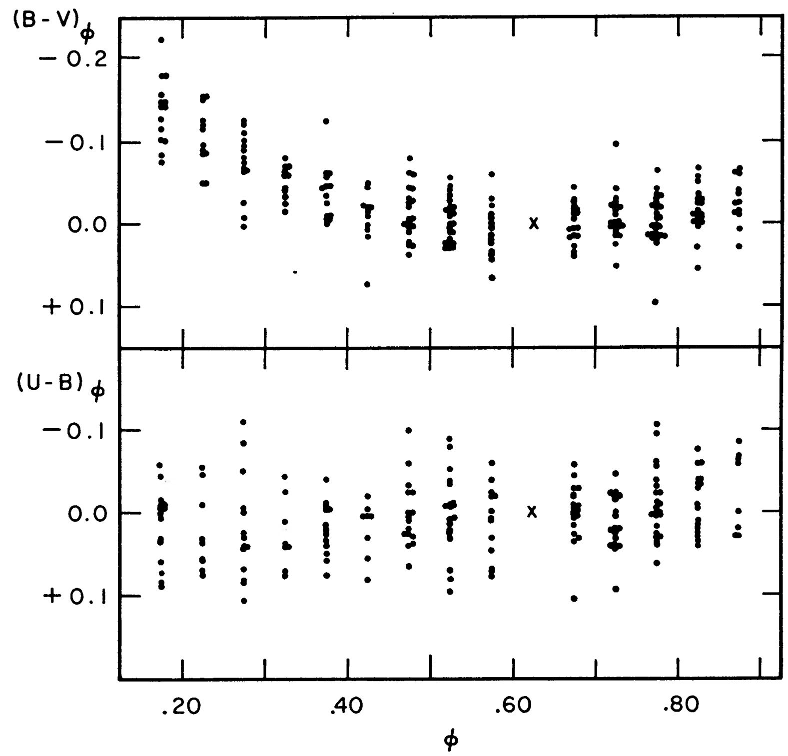

FIG. 1.—Differences in color index from the value in the phase interval $0^{P}.60 < \phi < 0^{P}.65$

formed at each interval of $0^{P}.05$ for which there were observations. Figure 1 is a plot of the differences, $(B - V)\phi$ and $(U - B)\phi$, between the color indices at any given phase interval and that in the interval $0.60 < \phi < 0.65$. Each point represents the difference found for an individual star. The average and the standard deviation of these differences were calculated for each phase interval and are listed in Table 2.

The average value of $B - V$ in each interval from $0^{P}.50$ to $0^{P}.80$ deviates by less than 0.01 mag. from the value in the interval $0^{P}.60 < \phi < 0^{P}.65$. The same deviation for $U - B$ is less than 0.02 mag. The scatter, as represented by the standard deviations, is about 0.03 mag. in $B - V$ and 0.04 mag. in $U - B$ and increases in the intervals closer to maximum light. An inspection of the individual light-curves that make up Figure 1 does not reveal any systematic departure from this average behavior.

An error in the observation in the interval $0^{P}.60 < \phi < 0^{P}.65$ produces a corresponding shift in all the $(B - V)_\phi$'s and $(U - B)_\phi$'s obtained for a given star. Also, many of the points in Figure 1 represent observations of faint stars so that photometric errors contribute greatly to the scatter. The first source of error is partially eliminated if we compare the observations in each phase interval to the average color index in the entire interval $0^{\mathrm{P}}.50 < \phi < 0^{\mathrm{P}}.80$. The second source of error is reduced by making these comparisons for a group of well-observed stars. For this purpose all the variables which are brighter than $m_V = 12.0$ at minimum light, which are north of $\delta = 10°$, and which were observed at least ten times in one season were chosen. Table 3 gives $(B - V)_\phi$ and $(U - B)_\phi$, redefined as the differences in color index from the average value during the interval $0^{\mathrm{P}}.50 < \phi < 0^{\mathrm{P}}.80$, for these selected stars.

To determine the dependence of color index upon period, the fifteen well-observed stars were divided into two groups with periods longer and shorter than $0^{\mathrm{d}}.5$. The average values of $(B - V)_\phi$ and $(U - B)_\phi$ for each of these groups are plotted against phase in

TABLE 2

DIFFERENCES IN COLOR INDEX FROM THE VALUE AT $0.60 < \phi < 0.65$

ϕ	$(B-U)_\phi$	σ	$(U-B)_\phi$	σ
0.15–0.20	−0.137	±0.039	+0.022	±0.040
.20– .25	− .100	± .034	+ .038	± .051
.25– .30	− .073	± .038	+ .021	± .061
.30– .35	− .051	± .020	+ .037	± .037
.35– .40	− .035	± .033	+ .018	± .036
.40– .45	− .009	± .031	+ .017	± .031
.45– .50	− .014	± .032	+ .001	± .040
.50– .55	− .007	± .026	.000	± .046
.55– .60	+ .009	± .030	+ .014	± .043
.60– .65	.000	± .000	.000	± .000
.65– .70	− .002	± .021	− .006	± .025
.70– .75	− .006	± .028	+ .018	± .034
.75– .80	− .003	± .029	− .009	± .043
.80– .85	− .014	± .027	− .005	± .036
0.85–0.90	−0.026	±0.027	−0.036	±0.042

TABLE 3

DIFFERENCES IN COLOR INDEX FROM THE AVERAGE VALUE DURING $0.50 < \phi < 0.80$ FOR A SELECTED GROUP OF STARS

ϕ	$(B-V)_\phi$	σ	$(U-B)_\phi$	σ
0.15–0.20	−0.138	±0.028	+0.039	±0.040
.20– .25	− .089	± .028	+ .038	± .037
.25– .30	− .071	± .023	+ .034	± .037
.30– .35	− .046	± .023	+ .023	± .015
.35– .40	− .028	± .022	+ .018	± .029
.40– .45	− .017	± .015	+ .011	± .025
.45– .50	− .001	± .011	+ .006	± .007
.50– .55	+ .005	± .016	− .008	± .023
.55– .60	+ .005	± .014	+ .004	± .008
.60– .65	+ .002	± .012	− .005	± .023
.65– .70	+ .002	± .008	+ .004	± .015
.70– .75	− .007	± .013	+ .003	± .021
.75– .80	− .003	± .019	− .006	± .019
.80– .85	− .011	± .015	+ .007	± .034
0.85–0.90	−0.055	±0.034	−0.043	±0.024

Figure 2. The group with $P < 0^d5$ days has a larger total range in $B - V$. It also seems to have a more nearly constant $B - V$ preceding minimum light. Extensive observations would be needed to prove whether the stars with $P > 0^d5$ days are really bluer at 0^P70 than at 0^P50 as the diagram indicates. In any case the total change in $B - V$ appears to be less than 0.03 mag. on the average, and the deviation from the average color in the entire interval even less.

It therefore seems reasonable to expect that the average value of $B - V$ in the interval $0^P50 < \phi < 0^P80$ can be estimated to within ± 0.03 mag. from a single observation anywhere within the interval provided, of course, that the photometry is accurate. For most problems in galactic research an RR Lyrae star can be considered to be constant in color during this interval. Multiple measurements should reduce the errors in color excesses to ± 0.01 mag. so that the uncertainty in RR Lyrae distance moduli would be essentially due to the uncertainty in their absolute magnitudes.

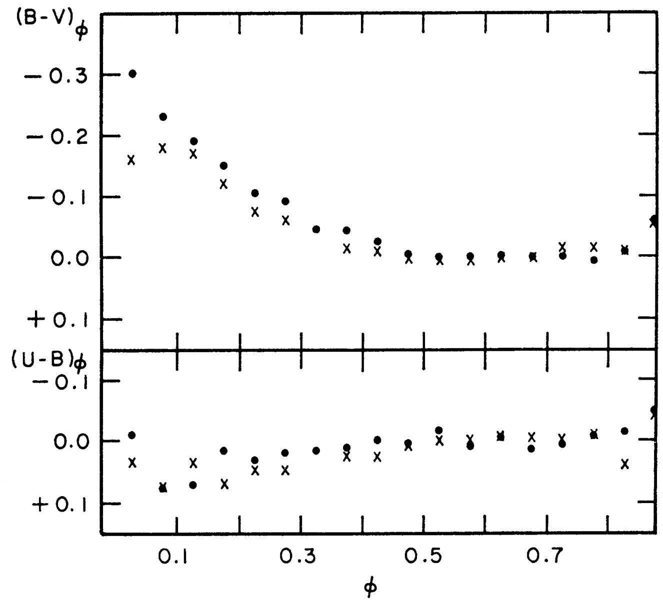

FIG. 2.—Difference in color index from the average value during the interval $0^P50 < \phi < 0^P80$. The data are taken from a group of well-observed stars as described in the text. The crosses and filled circles represent stars with $P > 0^d5$ and $P < 0^d5$, respectively.

The $U - B$ measurements show more scatter, but a tendency for the group with longer periods to have more of a depression in the ultraviolet after maximum is indicated. Preston and Paczynski (1964) noted that SW And and DX Del, both strong-lined stars, have small depressions. This observer found the same to be true of the strong-lined stars AT And and AR Per, but a pronounced depression is seen in KX Lyr, another example of this group. Near minimum light no large differences in $U - B$ are noted.

It was decided to use simply the average of all observations during the interval $0^P50 < \phi < 0^P80$ as a parameter to compare the various stars. In the discussion of the data in this survey, observations slightly outside this phase interval were included in this average when the data were sparse for a particular star. The observations used to form these averages are denoted with asterisks in Table 1. Throughout the rest of the paper the expressions $B - V$ and $U - B$ will refer to these average values listed in the fifth and sixth columns of Table 4. The number of observations making up the averages appears in the seventh column. The third column contains the period in days. The galactic latitudes and longitudes are taken from Plaut's (1963) catalogue. The other quantities in Table 4 will be explained later.

TABLE 4

MINIMUM LIGHT COLOR INDICES AND DERIVED QUANTITIES

	Star	P	ΔS	B-V	U-B	n	δ(U-B)	$(B-V)_c$	E_{B-V}	l^{II}	b^{II}
1.	SW And	0.442	0	0.531	0.180	5	0.148	0.420	0.134	116°	-33°.1
2.	XX And	.723	9	.455	-0.012	2	.010	.447	.094	128	-23.6
3.	AT And	.617	3	.569	0.107	3	.048	.533	.205	110	-18.1
4.	SX Aqr	.536	9	.416	.029	8	.080	.356	.047	058	-34.0
5.	TZ Aqr	.571	5	.464	.029	3	.045	.430	.113	053	-44.3
6.	YZ Aqr	.552	-	.476	.043:	3	.050:	.439:	.127:	049	-49.8
7.	BN Aqr	.470	(4)	.398:	---	1	---	---	---	056	-50.7
8.	BR Aqr	.482	3	.444	.073:	3	.103:	.368:	.072:	075	-65.2
9.	CP Aqr	.463	3	.512	.112	1	.093	.442	.151	049	-31.3
10.	AA Aql	.362	0	.460	.133	3	.152	.346	.079	043	-25.0
11.	341 Aql	.578	3	.454	.094	7	.117	.366	.047	046	-22.0
12.	X Ari	.651	10	.565	.066	8	.009	.558	.222	169	-39.8
13.	TZ Aur	.392	2	.470	.188	3	.200	.320	.046	177	20.9
14.	ST Boo	.622	-	.414	.051	4	.103	.337	.008	057	55.2
15.	SV Boo	.581	-	.444	.015	5	.045	.410	.091	069	65.5
16.	SW Boo	.513	(7)	.410	.031	4	.086	.346	.043	063	67.7
17.	TW Boo	.532	-	.412	0.045	6	.098	.339	.031	071	62.9
18.	UU Boo	.457	-	.391	-0.007	5	.061	.345	.055	056	58.0
19.	UY Boo	.651	(10)	.399	-0.006	4	.057	.356	.020	354	68.8
20.	RW Cnc	.547	-	.411	0.002	5	.056	.369	.058	197	43.5
21.	SS Cnc	.367	2	.513	.199	4	.180	.378	.110	199	26.3
22.	TT Cnc	.563	7	.483	.072	6	.074	.428	.113	212	28.4
23.	W Cvn	.552	7	.429	0.070	6	.111	.346	.034	072	71.0
24.	Z Cvn	.654	(8)	.401	-0.005	3	.056	.359	.022	124	73.3
25.	RR Cvn	.559	7:	.409	0.068	4	.124	.316	.002	154	81.1
26.	SW Cvn	.442	-	.384	.036	6	.110	.302	.016	135	79.8
27.	SZ Cvn	.550	-	.418	.027	2	.077	.360	.048	077	73.7
28.	RV Cap	.448	6	.430	.017	1	.057	.387	.099	033	-35.5
29.	RR Cet	.553	5	.445	.032	4	.062	.399	.086	143	-59.9
30.	RZ Cet	.511	4	.400	.011	3	.073	.345	.042	178	-60.3
31.	UU Cet	.606	4	.422	.019:	2	.065:	.373:	.048:	073	-75.1
32.	S Com	.587	7	.389	.021	6	.091	.321	.000	213	85.9
33.	V Com	.469	-	.400	.037	4	.099	.325	.032	209	80.8
34.	Z Com	.547	-	.442	---	4	---	---	---	328	80.6
35.	RY Com	.469	3:	.396	.034	4	.099	.321	.028	342	85.1
36.	UY Cyg	.561	3	.492	.108	12	.104	.416	.101	075	-09.6
37.	XZ Cyg	.467	6	.404	.065	9	.124	.311	.019	088	17.0
38.	DM Cyg	.420	0	.558:	.232	2	.180	.423:	.143	079	-12.4
39.	RW Dra	.443	3	.406	.063	5	.121	.315	.034	087	40.6
40.	XZ Dra	.476	3	.465	.132	4	.147	.355	.061	096	22.5
41.	AE Dra	.603	(4)	.449	.088	4	.115	.363	.038	084	25.4
42.	RX Eri	.587	9	.481	0.075	5	.079	.422	.101	214	-33.9
43.	SV Eri	.714	9	.444	-0.012	2	.019	.430	.079	194	-53.5
44.	UZ Eri	.649	-	.471	0.011	3	.022	.455	.119	199	-54.5
45.	BB Eri	.570	8	.413	0.045	3	.098	.340	.023	219	-34.4
46.	BK Eri	.354	-	.400	-0.056:	2	.006:	.396:	.131:	176	-51.7
47.	RR Gem	.397	3	.524	0.194	7	.167	.399	.124	187	19.5
48.	AK Gem	.529	-	.565	---	3	---	---	---	201	07.0
49.	GI Gem	.433	-	.467:	.137:	6	.151:	.353:	.069:	202	08.9
50.	TW Her	0.400	2	0.459	.178	4	0.198	0.311	0.035	056	24.8

TABLE 4 (Continued)

	Star	P	ΔS	B-V	U-B	n	δ(U-B)	$(B-V)_c$	E_{B-V}	l^{II}	b^{II}
51.	VX Her	0.455	5	0.428	0.074	5	0.116	0.341	0.052	035°	39°1
52.	VZ Her	.440	4	.411	.059	7	.113	.326	.040	060	34.6
53.	AR Her	.470	6	.353	.024	6	---	---	---	074	48.2
54.	BD Her	0.474	2	.626	.262	5	.161	.506	.212	048	07.6
55.	CE Her	1.209	7	.500	.031	3	---	---	---	039	22.0
56.	EE Her	0.496	-	.472	.109	4	.120	.382	.083	033	43.0
57.	EP Her	.426	-	.465	.089	6	.104	.387	.105	052	23.4
58.	OS Her	.396	-	.476	.175:	4	.182:	.340:	.065:	061	25.0
59.	OX Her	.757	6:	.440	.014	3	.047	.405	.043	065	25.4
60.	RR Leo	.452	8	.414	.083	2	.135	.313	.025	208	53.1
61.	RX Leo	.653	(5)	.455	.054	6	.076	.398	.061	209	70.5
62.	SS Leo	.626	-	.403	.024	4	.084	.340	.010	265	57.1
63.	ST Leo	.478	7	.403:	.077	4	.137:	.300:	.005:	253	66.1
64.	SU Leo	.472	-	.402	.030:	4	.091:	.334:	.041:	229	43.8
65.	WW Leo	.603	-	.462:	.072	4	.090:	.395:	.070:	226	38.4
66.	AA Leo	.599	-	.435	.052	4	.089	.368	.044	254	66.1
67.	V Lmi	.544	(4)	.405	.051	5	.109	.328	.017	201	57.8
68.	Y Lmi	.524	-	.404	.015	4	.075	.348	.042	194	56.0
69.	TT Lyn	.597	-	.439	.028	7	.062	.393	.070	176	41.6
70.	RZ Lyr	.511	9	.446	.058	6	.087	.381	.078	062	15.8
71.	AQ Lyr	.357	-	.561	.228	4	.174	.431	.165	055	15.2
72.	CX Lyr	.617	7:	.581	.136	2	.068	.530	.202	059	12.7
73.	IO Lyr	.577	3	.464	.102	3	.118	.375	.057	061	20.0
74.	KX Lyr	.441	0	.481	.159	6	.163	.359	.073	069	20.4
75.	ST Oph	.450	6	.618	.191	5	.096	.546	.258	023	16.6
76.	445 Oph	.397	1	.734	.407	5	.229	.562	.287	008	28.5
77.	452 Oph	.557	5:	.620	.193	6	.097	.547	.233	033	25.7
78.	CM Ori	.656	-	.661	.166	4	.040	.631	.294	200	-06.7
79.	VV Peg	.488	9	.423	0.000	6	.045	.389	.092	078	-30.4
80.	AE Peg	.497	7	.440	-0.008:	3	.025:	.421:	.122:	080	-33.9
81.	AO Peg	.547	1	.476	0.073	3	.080	.416	.105	070	-22.6
82.	AV Peg	.390	0	.515	.223	6	.203	.363	.089	077	-24.1
83.	BF Peg	.496	-	.434	.026:	2	.064:	.386:	.087:	089	-30.4
84.	CG Peg	.467	2	.534	.191	7	.157	.416	.124	077	-20.8
85.	DZ Peg	.607	-	.445	.040	2	.070	.393	.067	093	-41.4
86.	AR Per	.426	0	.775	.361	4	.153	.660	.378	155	-02.3
87.	RY Psc	.530	7	.456	---	2	---	---	---	101	-62.9
88.	VY Ser	.714	9	.438	.034	4	.069	.386	.035	006	44.1
89.	AN Ser	.522	0	.541	.271	4	.232	.367	.062	024	45.2
90.	AT Ser	.747	9	.438	.050	4	.085	.374	.015	018	42.5
91.	AV Ser	.488	(6)	.521	.206	4	.181	.385	.088	011	36.8
92.	AW Ser	.597	7:	.438	.031	3	.066	.389	.066	029	43.4
93.	CS Ser	.527	(6)	.411	.031	4	.086	.347	.041	007	45.4
94.	SS Tau	.369	-	.681	.274:	2	.134:	.581:	.312:	180	-38.5
95.	U Tri	.447	2	.449:	.170	3	.197:	.301:	.014:	138	-27.2
96.	TU Uma	.558	6	.414	.015	5	.067	.364	.050	199	71.9
97.	UU Vir	.476	2	.409	.076	3	.132	.310	.016	281	60.5
98.	UV Vir	.587	-	.412	.066	5	.119	.323	.002	287	62.3
99.	AS Vir	.553	-	.421	.048	3	.095	.350	.037	303	52.6
100.	AT Vir	.526	-	.398	.032	6	.096	.326	.020	305	57.4
101.	BC Vir	.565	-	.418:	.088:	2	.138:	.315:	.000:	323	67.5
102.	BN Vul	0.594	6	0.846	0.332	8	0.073	0.791	0.468	059	03.4

TABLE 4 (Continued)

Data from Other Observers

	Star	P	ΔS	B-V	U-B	n	δ(U-B)	$(B-V)_c$	E_{B-V}	l^{II}	b^{II}
103.	DX Del	0.473	2	0.541	0.176		0.137	0.438	0.145	058°	-18°8
104.	SU Dra	.660	10	.431	.000		.040	.401	.063	133	48.3
105.	TV Leo	.673	10	.426	.05 :		.093:	.356:	.014:	263	49.1
106.	RR Lyr	0.567	6	0.440	0.036		0.069	0.388	0.072	075	12.3
					Southern Hemisphere	(Kinman)					
107.	WY Ant	0.574	6	0.449	---	17	0.089	0.382	0.064	267	22.1
108.	S Ara	.452	3	.467	---	3	.112	.383	.095	343	-12.4
109.	IU Car	.737	9	.525	---	23	.062	.479	.118	270	-23.0
110.	BI Cen	.453	2	.603	---	22	.170	.476	.187	295	02.3
111.	499 Cen	.521	6	.465	---	15	.089	.398	.093	315	18.1
112.	RY Col	.479	3	.434	---	12	.112	.350	.055	246	-35.0
113.	SW Cru	.328	0	.796	---	5	.176	.664	.406	296	01.9
114.	RX Eri	.587	6	.494		17	.089	.427	.106	214	-33.9
115.	SW For	.804	10	.443	---	3	.050	.406	.034	243	-60.8
116.	FY Hya	.637	7	.430	---	10	.081	.369	.036	319	31.4
117.	UV Oct	.543	9	.481	---	23	.062	.435	.125	308	-23.5
118.	TY Pav	.710	10	.528	---	5	.050	.491	.141	331	-17.1
119.	DN Pav	.468	(8)	.390	---	2	.097	.317	.025	333	-30.8
120.	RV Phe	.595	(8)	.428	---	5	.097	.355	.032	336	-64.0
121.	675 Sgr	.642	11	.451	---	16	.010	.445	.111	358	-07.8
122.	494 Sco	.427	(2)	.548	---	8	.170	.421	.139	357	-00.5
123.	W Tuc	.642	(7)	.399	---	8	.081	.338	.004	302	-53.7
124.	YY Tuc	0.635	(8)	0.44	---	3	0.097	0.367	0.035	325	-52.2

Table 4 includes a number of stars from other observers. These are: DX Del, Preston (1961); SU Dra, Spinrad (1961); TV Leo, Paczynski (1963); and RR Lyr, Hardie (1955). The last eighteen stars are from the southern hemisphere survey of Kinman (1961). The colors listed are the average of all the published observations from $0^{P}.50$ to $0^{P}.80$. One star, RX Eri, is in common between the present survey and Kinman's. Kinman's observations in this phase interval are 0.013 mag. redder in $B - V$. Paczynski's data for RX Eri (Preston and Paczynski 1964), obtained the season before at the Crossley, give results that are more negative by 0.017 mag. in $B - V$ and 0.009 mag. in $U - B$ than those obtained in the present survey. These stars from other observers are included in all the discussions that follow.

b) *Line-blanketing and Period Relations*

Figure 3 is a plot of $B - V$ versus $U - B$ for all the stars in the survey. The curved line is the relation for the main sequence of the Hyades (Sandage and Eggen 1959, Table III). Three different symbols have been used to denote different period groups.

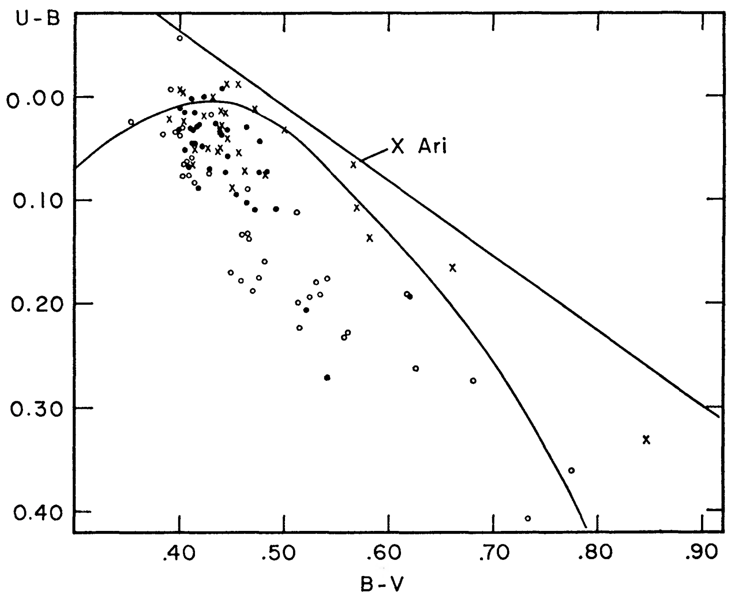

FIG. 3.—The observed $U - B$, $B - V$ diagram for RR Lyrae stars near minimum light. The curved line represents the main sequence of the Hyades. The straight line is an interstellar reddening line with a slope of 0.72. Open and filled circles represent stars with $P < 0^{d}.48$ and $0^{d}.48 < P < 0^{d}.58$, respectively. The crosses represent stars with $P > 0^{d}.58$.

The intrinsic UBV colors of a star are influenced by its temperature, line-blanketing, and surface gravity. The effect of interstellar reddening is to move the position of the star downward and to the right in the $U - B$, $B - V$ diagram, an effect, clearly seen in the few RR Lyraes in Figure 3 having large values of $B - V$ and $U - B$. The majority of the stars, which are less affected by reddening, lie in the region $0.4 < (B - V) < 0.5$ but show roughly twice this range in $U - B$. This large vertical dispersion cannot be attributed to differential interstellar reddening. Since the variables most deficient in the ultraviolet tend to be those with the shortest periods, we further conclude that this inhomogeneity is related to period.

A relation between $B - V$ and period is obtained from Figure 4 which contains those stars with $|b^{II}| > 50°$. We assume that the stars at such high galactic latitudes are little affected by differential interstellar reddening. However, Figure 5, in which $U - B$ is plotted against period for the same stars, again shows a large dispersion in $U - B$. The photometric errors discussed in § II cannot account for the scatter. We therefore conclude that even this high-latitude sample is inhomogeneous.

Preston (1959) has demonstrated that a correlation between period and line strength exists. Line blanketing in $B - V$ is not negligible (Preston 1961). So if the scatter in $U - B$ is at least partially attributable to differential line blanketing, the line-free $B - V$ color index, $(B - V)_c$, probably does not have the same dependence on period that is found for the observed color index, $B - V$. If possible, we should correct for differential line blanketing before obtaining a color-period relation.

A number of blanketing estimates for RR Lyrae stars have been made from high dispersion spectrograms (Preston 1961; Oke, Giver, and Searle 1962; and Sturch 1963). The corrections for $B - V$, the $\Delta(B - V)$'s listed in Table 5, are thought to be fairly accurate, but those for $U - B$ are probably unreliable. The spectrograms do not cover the entire region of the U filter, the stellar continuum is difficult to find in strong-lined stars, and the effect of the converging Balmer lines is difficult to assess. Therefore, the slope

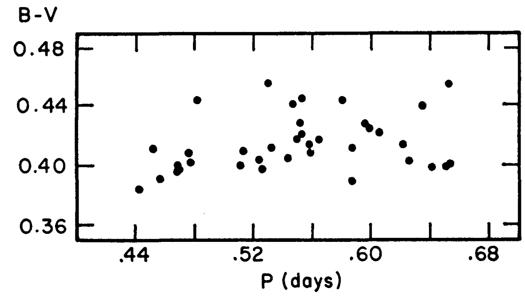

FIG. 4.—Observed $B - V$ versus period for stars with $|b^{II}| > 50°$

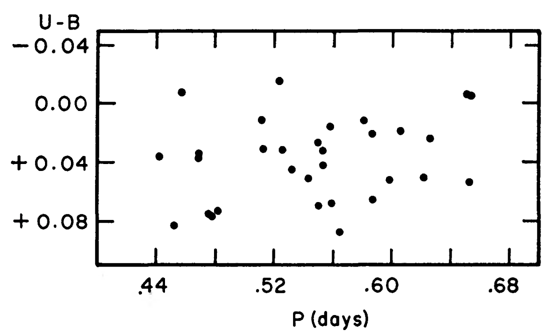

FIG. 5.—Observed $U - B$ versus period for stars with $|b^{II}| > 50°$

TABLE 5

LINE-BLANKETING EFFECTS

Star	P (days)	$\Delta(B-V)$	$\delta(U-B)$
X Ari	0.651	−0.01	0.009
SU Dra	.660	+ .04	.040
RR Lyr	.567	+ .04	.069
DX Del	.473	+ .10	.137
SW And	0.442	−0.11	0.148

of the blanketing line, i.e., the line in the $U - B$, $B - V$ plane along which the line-free colors are shifted as the intensity of the metallic lines increases, is unknown.

The line-blanketing estimate for X Ari is the smallest of those listed in Table 5. The observed $B - V$ and $U - B$ of X Ari should be nearly equivalent to the line-free $B - V$ and $U - B$ of an RR Lyrae with a period of $0^{d}65$, except for the effect of interstellar reddening. The straight line in Figure 3 is an interstellar-reddening line that passes 0.01 mag. above the observed position of X Ari. The intrinsic line-free colors of X Ari should lie somewhere on this line. Intrinsic line-free colors of the other RR Lyrae stars should lie close to this line also, except that, as seen from Figure 4, the $B - V$'s of the shorter-period stars are probably slightly bluer. The vertical displacement of the observed color indices from this line, $\delta(U - B)$, gives an indication of the amount of line blanketing present.

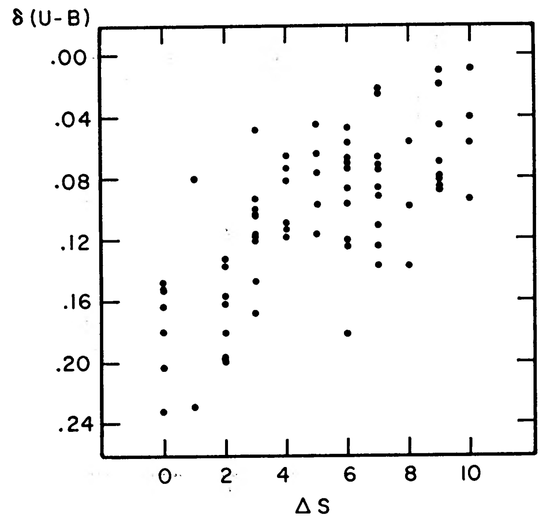

FIG. 6.—The correlation of $\delta(U - B)$ with ΔS

This reddening line is given by the equation

$$U - B = -0.35 + 0.72\,(B - V)\,, \tag{1}$$

and $\delta(U - B)$ is defined as

$$\delta(U - B) = (U - B) - [-0.35 + 0.72(B - V)]\,, \tag{2}$$

where $(U - B)$ and $(B - V)$ are the observed values.

The slope of this line, $E_{U-B}/E_{B-V} = 0.72$, is the same as that usually given for O-type stars although the second-order term, $0.05\,E_{B-V}$ has been omitted. Wampler (1961) has suggested that the second-order term might be simply the result of combining observations from different galactic longitudes where the reddening slope differs. Fernie (1963) found a slope of 0.71 ± 0.01 with no evidence for a second-order term for F-type supergiants. From the concentration of points near $B - V = 0.4$ in Figure 3 it would appear that few of the stars in the survey are reddened more than 0.2 mag., so the effect of the second-order term would be less than 0.01 mag. for most of the stars.

A strong correlation should exist between $\delta(U - B)$ and ΔS (Preston 1959) since both are measures of line strength. The quantity ΔS is the difference in tenths of a spectral type of an RR Lyrae at minimum light as judged from the Ca II K line and the hydrogen lines. It varies from 0 (strong-lined) to 11 (weak-lined). Figure 6 is a plot of $\delta(U - B)$ versus ΔS for those stars for which both quantities have been observed. Preston estimates the error in obtaining ΔS at around 2, and the error in $\delta(U - B)$ is at least 0.02 mag. Much of the scatter can therefore be explained by the observational errors involved.

The quantity $\delta(U - B)$ has been introduced to provide a photometric parameter suitable for estimating the line blanketing in $B - V$. Before we proceed to use it in determining intrinsic colors for the RR Lyrae stars, it should be noted that the parameter $\delta(U - B)$ may prove to be as useful as the information on intrinsic colors (see § IV).

The $\delta(U - B)$'s for the five stars of Table 5 are plotted against their $\Delta(B - V)$'s in Figure 7. The value of $\delta(U - B)$ seems to be a smoothly increasing function of $\Delta(B - V)$. The relation

$$\delta(U - B) = \tfrac{4}{3}\Delta(B - V) \tag{3}$$

represents the data well.

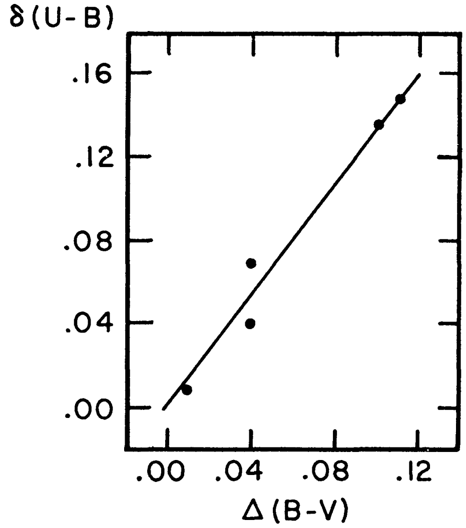

FIG. 7.—The relation between $\delta(U - B)$ and $\Delta(B - V)$

The equation

$$(B - V)_c = B - V - \tfrac{3}{4}\delta(U - B) \tag{4}$$

is used to obtain $(B - V)_c$, the $B - V$ color index free from blanketing due to the metallic lines. This quantity is tabulated in the ninth column of Table 4. In Figure 8, $(B - V)_c$ is plotted against period for the stars with galactic latitude $b^{\mathrm{II}} \geq 56°$. Cosecant b varies by only 0.2 for these stars, and the elimination of the southern stars assures that any differences in the total amount of interstellar reddening between the two galactic poles is not introduced.

The line in Figure 8 is the least-squares solution obtained for the data

$$(B - V)_c = 0.21 + 0.24\, P\ (\text{days}) \pm 0.03 \pm 0.05\ (\text{p.e.})\,. \tag{5}$$

The probable error of the individual $(B - V)_c$'s is less than 0.02 mag.

c) *Interstellar Reddening and Intrinsic Colors*

Before the intrinsic colors of RR Lyrae stars can be found, an estimate of the interstellar reddening at the galactic poles must be obtained. If the RR Lyrae stars in high galactic latitudes have sufficiently large z distances that they lie above the dust associated with the plane, a cosecant reddening law may be employed for this purpose.

Extensive use has been made of a model of the galactic dust layer that assumes an exponential decrease in the coefficient of selective absorption with increasing z (e.g., Williams 1934). If the selective absorption is represented by

$$c(z) = c_0 \exp(-z/\beta), \tag{6}$$

where c_0 and β are constants and $z = r \sin b$, it follows that the reddening for a given object is

$$E = \frac{c_0 \beta}{\sin b}\left[1 - \exp\left(-\frac{r \sin b}{\beta}\right)\right]. \tag{7}$$

For large values of $(r \sin b/\beta)$, equation (7) reduces to a simple cosecant law. Let us investigate the values of the exponential term in equation (7) for the stars in this survey with $b > 20°$. We assume that $M_V = 0.5$ for an RR Lyrae star. The m_V's are approximated by subtracting 0.5 mag. from the values found at minimum light, and no correction is made for interstellar absorption. Stibbs (1955) has reviewed the work of Oort, Parenago, and van Rhijn, and finds values of β that range between 100 and 124 pc. Other values of β have been found in specific directions: 187 pc at the north equatorial pole

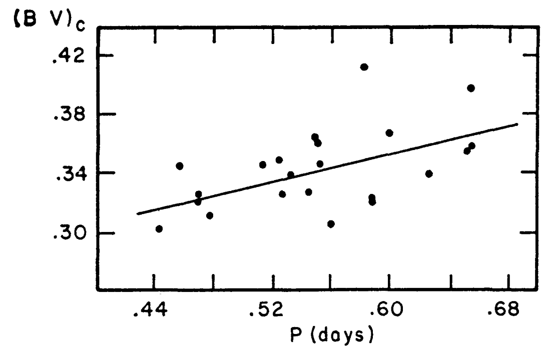

FIG. 8.—The relation between $(B - V)_c$ and period for stars with $b^{\text{II}} > 56°$

(Abt and Golso 1962); 140, 82, and 83 pc toward the center and anticenter of the Galaxy (Arp 1965). The average of these determinations agrees well with the highest value reported by Stibbs, so we use $\beta = 124$ pc. The largest value found for exp $(-\, r \sin b/\beta)$ is that for XZ Dra, 0.08. Four other stars have values close to 0.05; the rest have values smaller than 0.05. Therefore omission of the exponential term would introduce errors of less than 5 per cent in a reddening law determined from stars in this survey with $b > 20°$.

Arp (1962) has suggested the possibility of reddening material at large z distances. Such material might be detectable from the color indices of RR Lyrae stars with $b \geq 56°$. To eliminate any differences due to line blanketing we use the $(B - V)_c$ index for this purpose. The period dependence has been removed by adding 0.24 ΔP to each $(B - V)_c$, where ΔP is the difference, $0.65 - P$ (days). The result, $(B - V)_{c,p}$, is plotted against m_V at minimum light in Figure 9. The least-squares solution for these data gives a slope of 0.005 m_V, or an increase of around 0.02 mag. in the color index from the brightest to the faintest of these stars. However, if the $(B - V)_{c,p}$ for SV Boo (which is 0.03 mag. redder than the value for any other star) is not considered in the solution, the slope is reduced to 0.0015, an increase of only 0.006 mag. in $(B - V)_{c,p}$ for the magnitude range of these data. Using the same assumptions as before, the distances of these stars (which closely correspond to their z distances) range from 0.7 to 4 kpc. We conclude that there is little evidence for additional reddening. (The same conclusion can be drawn from the observed $B - V$'s, uncorrected for period or line blanketing.)

From the above analysis it seems reasonable to use the RR Lyrae stars in this survey to determine a cosecant reddening law. We again use the line-free color index, $(B-V)_c$, for this purpose and include all stars with $|b| > 20°$ (csc $b < 2.9$). Solutions for both galactic caps, including both period and coescant terms, are

north galactic cap:

$$(B-V)_c = \underset{\pm 0.03}{0.21} + \underset{\pm 0.05}{0.17}\, P\,(\text{days}) + \underset{\pm 0.01\ \text{p.e.},}{0.04}\, \csc b$$

south galactic cap:

$$(B-V)_c = \underset{\pm 0.04}{0.21} + \underset{\pm 0.06}{0.12}\, P\,(\text{days}) + \underset{\pm 0.01\ \text{p.e.}}{0.01}\, \csc b$$

The period terms are appreciably smaller in these solutions than in equation (5) for the stars with $b \geq 56°$. These solutions do not take into account well-known effects of longitude upon interstellar reddening. If the color indices are examined with respect to longitude, it becomes apparent that the stars in the Taurus and Ophiuchus regions are

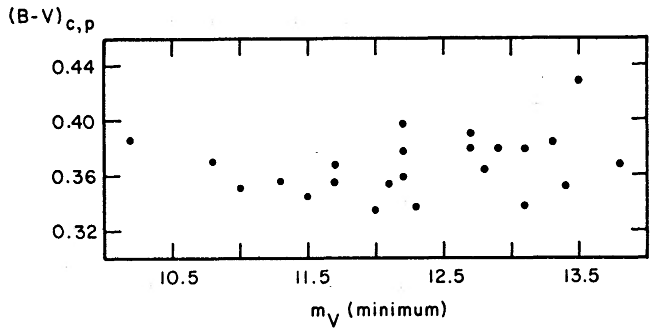

FIG. 9.—The $B-V$ color index, corrected for both line blanketing and period, versus m_V near minimum light for stars with $b > 56°$.

excessively reddened. Stars like X Ari ($P = 0\overset{d}{.}65$) and SS Tau ($P = 0\overset{d}{.}37$), representative of the extremes in period in this survey, are included in these regions, resulting in a smaller coefficient for the period term in a least-squares solution. If these reddened regions are omitted (but stars with $b > 70°$ are kept) the following solutions are obtained:

north galactic cap, $45° < l^{\text{II}} < 360°$:

$$(B-V)_c = \underset{\pm 0.02}{0.19} + \underset{\pm 0.03}{0.24}\, P\,(\text{days}) + \underset{\pm 0.01\ \text{p.e.}}{0.02}\, \csc b$$

south galactic cap, $0° < l^{\text{II}} < 100°$, $210° < l^{\text{II}} < 360°$:

$$(B-V)_c = \underset{\pm 0.04}{0.23} + \underset{\pm 0.05}{0.19}\, P\,(\text{days}) + \underset{\pm 0.01\ \text{p.e.}}{0.03}\, \csc b$$

Another solution avoids much of the reddened area. It is the one for all stars with $b > 30°$:

north galactic cap, $b > 30°$, all longitudes:

$$(B-V)_c = \underset{\pm 0.02}{0.15} + \underset{\pm 0.03}{0.24}\, P\,(\text{days}) + \underset{\pm 0.01\ \text{p.e.}}{0.05}\, \csc b$$

The period terms in these solutions that avoid heavily reddened regions all agree well with each other and with equation (5). The probable errors of these solutions are generally smaller also. We therefore adopt the average of these solutions, 0.03 mag., for the reddening at the poles and the following equation for the intrinsic, line-free color index of an RR Lyrae:

$$(B-V)_{0,c} = 0.18 + 0.24\, P\,(\text{days}) . \tag{8}$$

We now define the color excess, E_{B-V}, as the difference between the observed $B - V$ corrected only for blanketing and the intrinsic, line-free $B - V$ as calculated from equation (8). Thus,

$$E_{B-V} = (B - V)_c - (B - V)_{0,c} . \tag{9}$$

The values of E_{B-V}, calculated in this manner, may be found in the tenth column of Table 4.

Assuming that $E_{U-B}/E_{B-V} = 0.72$, then

$$(B - V)_0 = B - V - E_{B-V}, \text{ and} \tag{10}$$

$$(U - B)_0 = U - B - 0.72\, E_{B-V} , \tag{11}$$

where $(B - V)_0$ and $(U - B)_0$ are the intrinsic color indices corrected for reddening but not for blanketing, $B - V$ and $U - B$ are the observed values near minimum light, and the E's are the color excesses from equation (9).

By combining equations (2), (4), (8), (9), (10), and (11), the intrinsic color indices of RR Lyrae stars at minimum light are

$$(B - V)_0 = -0.54\, B - V + 0.75\, U - B + 0.24\, P\,(\text{days}) + 0.44 , \tag{12}$$

$$(U - B)_0 = -1.11\, B - V + 1.54\, U - B + 0.17\, P\,(\text{days}) + 0.32 . \tag{13}$$

The internal accuracy of equations (12) and (13) may be judged from Figure 10, a $(U - B)_0$, $(B - V)_0$ diagram for those stars with observed ΔS values. The open, half-filled, and filled circles represent ΔS values of 6–10, 4–5, and 0–3 respectively. The increasing value of ΔS with increasing ultraviolet excess is easily discerned. The straight line through these points is the least-squares solution for all the RR Lyrae stars with UBV photometry regardless of whether they have observed ΔS values. Its equation is

$$(B - V)_0 = 0.37 + 0.35\, (U - B)_0 \tag{14}$$

and the probable error of a single determination is 0.008 mag. The slope of this solution is not due to line blanketing alone since the line-free index, $(B - V)_c$, is dependent on period. Also it is well known that the position of a star in this portion of the $U - B$, $B - V$ diagram is sensitively dependent upon its surface gravity as seen in the three curved lines in Figure 10 which represent the empirical relations for the Hyades main sequence and for stars 1.0 and 2.0 mag. above the Hyades (Eggen and Sandage 1964). A surface gravity or luminosity effect that is correlated with line strength or period would be difficult to distinguish by UBV photometry alone. Perhaps an intermediate band-width system such as Strömgren's (1963) could be used for this purpose. We can, however, determine whether it is reasonable to attribute the range of $(U - B)_0$ to line blanketing alone. Preston (1961) found DX Del to have 0.19 mag. more line blanketing than X Ari in $U - B$. The result was uncertain for the reasons stated above, but compares favorably with the difference of 0.17 mag. in $(U - B)_0$ found in this study.

A diagram similar to Figure 10 can be drawn which indicates individual ΔS values. Considerable overlapping of ΔS values occurs in any interval of $(U - B)_0$ in such a diagram. However, it is possible to explain this overlapping from the errors in assigning

ΔS values. A differential luminosity effect in the RR Lyrae stars may still be present, but it is not needed to explain either the total range in $(U - B)_0$ or the overlapping of ΔS values.

d) Peculiar Stars

Two of the stars in this survey, AR Her and BK Eri, have anomalous colors. The peculiarity of AR Her is best seen from its position in Figure 3. It is 0.03 mag. bluer in

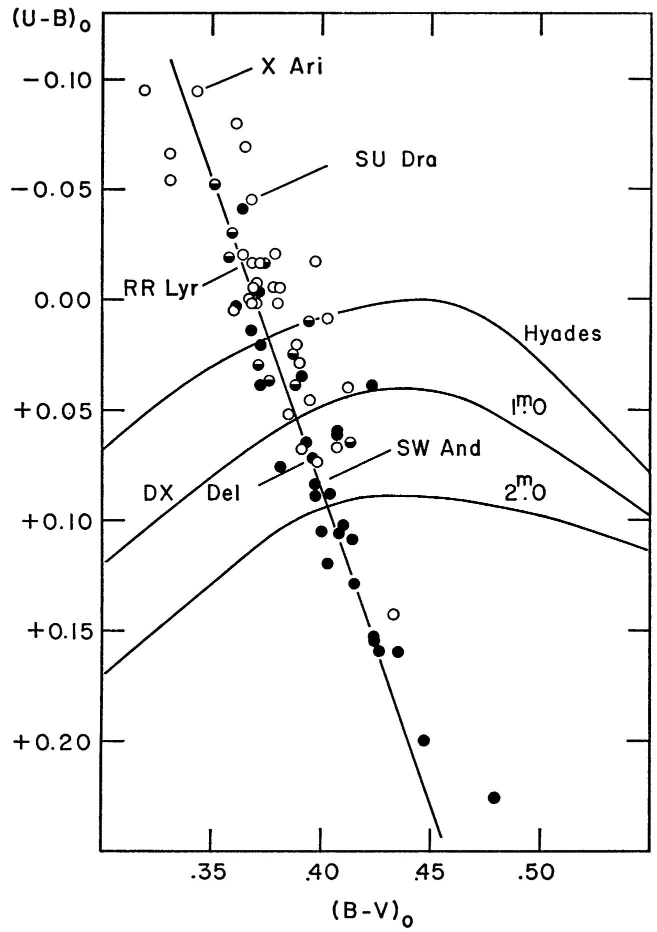

FIG. 10.—The $(U - B)_0$, $(B - V)_0$ diagram for those stars with observed ΔS values. The open, half-filled, and filled circles represent ΔS values of 6–10, 4–5, and 0–3, respectively. The straight line is the least-squares solution for all stars with UBV photometry. Also shown are the relations for the Hyades main sequence and for stars 1.0 and 2.0 mag. brighter than the Hyades.

$B - V$ than any other variable in the survey and 0.06 mag. bluer than would be predicted from the intrinsic color relation and its galactic latitude. This star was observed during the $0^P.50$ to $0^P.80$ phase interval a total of six times on three nights. It is therefore reasonable to assume that its blueness cannot be attributed to observational error alone. Preston (1959) noted that AR Her is one of a few stars in the period interval $0^d.44$ to $0^d.48$ which has systematically stronger hydrogen lines at minimum light than all the other Bailey type a's. Stronger hydrogen lines would indicate a higher temperature resulting in a smaller $B - V$ index.

A spectrogram of AR Her has been obtained by Preston at the coudé spectrograph of the 120-inch reflector. The dispersion was 48 Å/mm and the exposure time was 96 min beginning at JD 2438576.810. The approximate phase interval covered was from $0^P.67$ to $0^P.81$. A similar 4-min exposure of RR Lyr was made on the same plate immediately thereafter; it was near $0^P.70$ at the time. Direct-intensity microphotometer tracings indicate that the hydrogen lines in AR Her were stronger than those in RR Lyr. Comparisons of the Hγ profiles of each star were made with the theoretical profiles of Searle and Oke (1962). As Searle and Oke found, the profile for $\theta_e = 0.83$ ($\theta_e = 5040/T_e$) and $\log g = 1.5$ agreed well with the observed profile for RR Lyr. The same type of agreement was achieved for AR Her only when profiles for smaller θ_e were used. The best fit for AR Her was for $\theta_e = 0.80 \pm 0.02$.

A relation between the $B - V$ index and θ_e was developed by Preston and Paczynski (1964), but this relation did not include the effects of line blanketing. A maximum light the observed $B - V$ is affected only by interstellar reddening since line blanketing is negligible. Near minimum light both sources of reddening are present. The quantity θ_e was determined both at maximum and minimum light for five stars by Preston and Paczynski. Their results are listed in the second and third columns of Table 6. The intrinsic, unblanketed color indices at minimum as determined from equation (8) are listed in the fourth column. The $B - V$'s at maximum as observed by Paczynski are given in

TABLE 6

TEMPERATURES AND COLORS OF RR LYRAE STARS

Star	θ_e min.	θ_e max.	$(B-V)_{0,c}$	$B-V_{\max}$	E_{B-V}	$(B-V)_0$ max.
SW And......	0.85	0.68	0.286	0.20	0.13	0.07
X Ari.........	.83	.66	.336	.30	.22	.08
RR Cet.......	.83	.70	.313	.16	.09	.07
RX Eri.......	.84	.68	.321	.24	.10	.14
TU Uma......	0.84	0.68	0.314	0.17	0.05	0.12

the next column. The sixth column contains the color excesses as determined in this paper from which are obtained the intrinsic colors at maximum light. The relation between θ_e and the intrinsic, line-free $B - V$ index can be seen in Figure 11. If the points at the extremes of the relation are averaged, the following equation is obtained:

$$(B - V)_{0,c} = -0.83 + 1.36\, \theta_e\,. \tag{15}$$

Using this relation the predicted color of AR Her at minimum light is

$$(B - V)_{0,c} = 0.26 \pm 0.03\,.$$

The color predicted from equation (8) is $(B - V)_{0,c} = 0.29$.

It is therefore possible to explain the observed discrepancy in $B - V$ in terms of θ_e derived from the Hγ profile. The cause of the higher temperature, however, remains unknown.

It should be noted that the reason the anomalous color of AR Her was discovered is that it lies in an area that is not heavily reddened. If it had had a large color excess the position of this object in Figure 3 would not have seemed unusual. There are about thirty stars making up the envelope of the bluest variables in the survey indicating that as high as 3 per cent of the RR Lyrae stars may have colors similar to AR Her.

The other obviously peculiar star in the survey is BK Eri. From its short period ($P = 0^d.354$) one would expect it to be a strong-lined star. Its $\delta(U - B)$, however, is similar to that of X Ari. Subsequent observations in the autumn of 1964 have confirmed the ultraviolet excess for this star and have failed to indicate any large departure from the published period. It is definitely a type *a* RR Lyrae: an increase of 1.0 mag. in m_V in roughly 15 per cent of the period has been observed.

Since BK Eri has the shortest period of any star in the survey having *UBV* photometry, it may belong to another class of objects. A star with a slightly longer period, AQ Lyr ($P = 0^{d}357$), has a typically large $\delta(U - B)$. Other stars with shorter periods should be investigated to determine whether BK Eri is abnormal or simply representative of another type of variable.

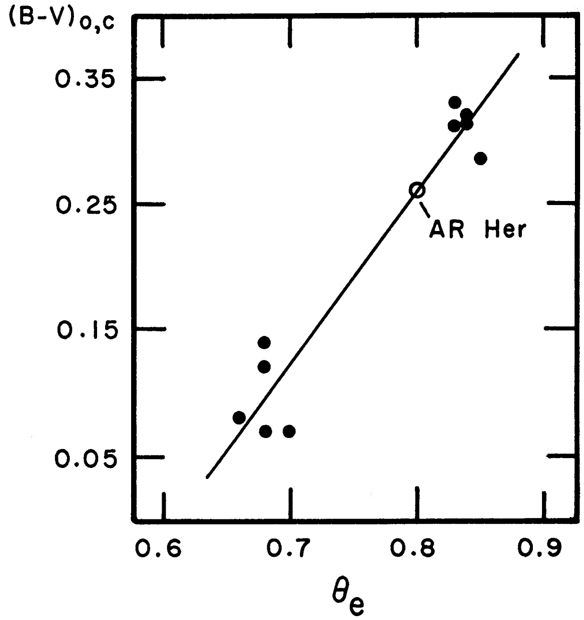

FIG. 11.—The $B - V$ index, corrected for line blanketing and reddening, versus $\theta_e(=5040/T_e)$ at minimum and maximum light.

IV. APPLICATIONS

a) Interstellar Reddening

The few O and B stars that exist at large *z*-distances are often peculiar and do not follow the intrinsic color relations. Later-type stars abound in these regions but are of little use as reddening indicators. The reason for this is illustrated quite effectively in Figure 12, the $U - B$, $B - V$ diagram for the comparison stars used in this survey with $|b| > 30°$. The solid line is the Hyades relation according to Sandage and Eggen (1959). The dotted line is the main sequence of nearby stars taken from Johnson and Morgan (1953). The data seem to fit the latter relation better, although there are numerous stars with ultraviolet excesses. Similar ultraviolet excesses were found for stars near the north galactic pole by Slettebak, Bahner, and Stock (1961). These authors found that the metallic lines in these objects are very weak and classified the spectra as those of F- and G-type subdwarfs. It would be extremely difficult to separate the effects of differential line blanketing and interstellar reddening for these stars by *UBV* photometry alone.

The integrated colors of galaxies and globular clusters have also been used to determine reddening at high latitudes. Besides the inherent difficulties of photometry of extended objects, the lack of precise intrinsic color relations for clusters and galaxies limits the accuracy of this method. As we have seen in this paper, however, accurate intrinsic colors of RR Lyrae stars can be defined.

The study of absorption in these areas has been confined to counts of galaxies. This is a statistical approach at best because of the irregularities in the distribution of galaxies.

The fine structure of the absorbing and reddening material cannot be determined from either galaxies or clusters, but it may be possible to make such a determination from RR Lyrae stars. These stars, which occupy the Hertzsprung gap, have a very low space density; however, their distribution extends to many kiloparsecs above the galactic plane. The number of RR Lyrae stars in the galactic caps is of the order of one per square degree brighter than $m_{pg} = 18$ (Kinman 1963). This coverage compares favorably with the several square degrees which are usually averaged to obtain reliable information from galaxy counts.

Crude maps of interstellar reddening may be made from even the small sample of stars in this survey. Figures 13 and 14 are such maps of the northern and southern galactic hemispheres. The galactic poles are in the center and the numbers are the E_{B-V}'s in hundredths of a magnitude. Underlined numbers are from the southern survey of

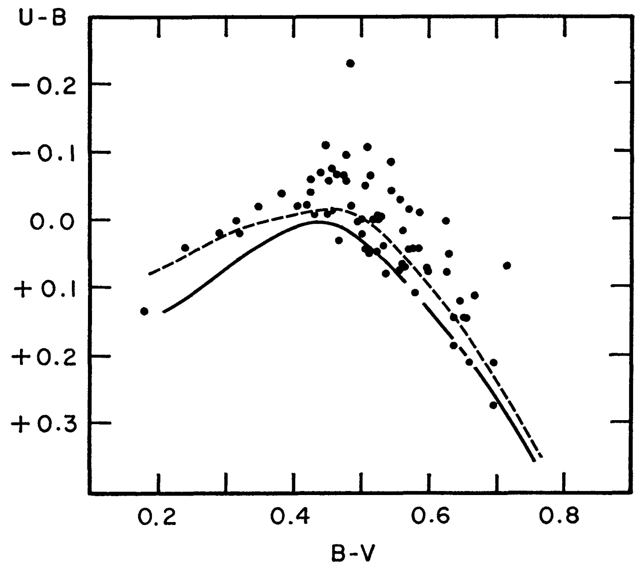

FIG. 12.—The $U - B$, $B - V$ diagram for the comparison stars with $|b| > 30°$. The solid line is the relation for the Hyades. The dashed line is the main sequence of nearby stars (Johnson and Morgan 1953).

Kinman. Attention is called to the four circled stars in Taurus and Ophiuchus which are reddened about 0.1 mag. more than any other stars at comparable latitudes. It will also be noticed that the southern stars observed by Kinman show smaller color excesses than those southern stars observed from the northern hemisphere. This could well be a longitudinal effect in the distribution of the dust or it could be due to systematic differences in observing and analysis. Line-blanketing estimates for the southern stars were based on Kinman's ΔS values instead of $\delta(U - B)$'s. However, the color excesses derived for RX Eri, the one star in common between the two surveys, agree within 0.01 mag.

Dr. C. D. Shane has kindly permitted me to examine a list of corrected and smoothed galaxy counts divided into small galactic areas. The absorption, derived from these data using the equation

$$A_{pg} = 1.95 - \log N/0.5 \csc b \,, \tag{16}$$

agrees in general with the color excess in this survey in the sense that increased absorption is accompanied by increased reddening. However, the amount of absorption found by Shane is much greater than would be expected from the reddening found in this survey. Shane (1964) finds $A_{pg} = 0.48$ mag. at the galactic poles, which would lead to $E_{B-V} = 0.12$ mag. if the commonly accepted ratio of total to selective absorption is used.

While a comparatively large value for the total absorption has been found, there is

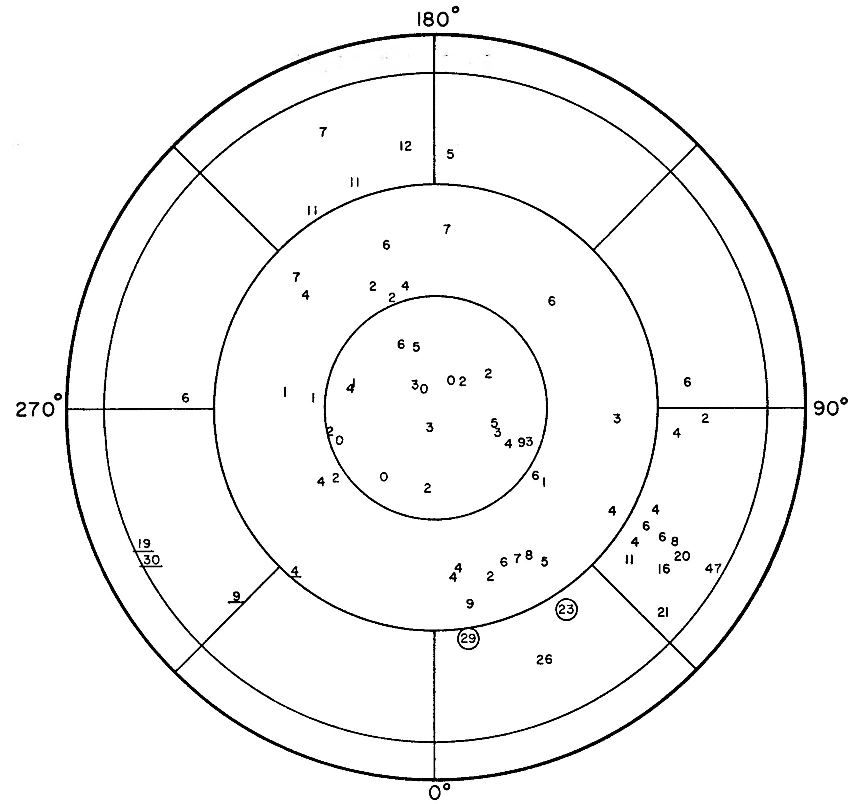

FIG. 13.—The color excess, E_{B-V}, in hundredths of a magnitude for stars in the north galactic hemisphere. The north galactic pole is at the center of the diagram. Latitudes 60°, 30°, and 0° are indicated by concentric circles.

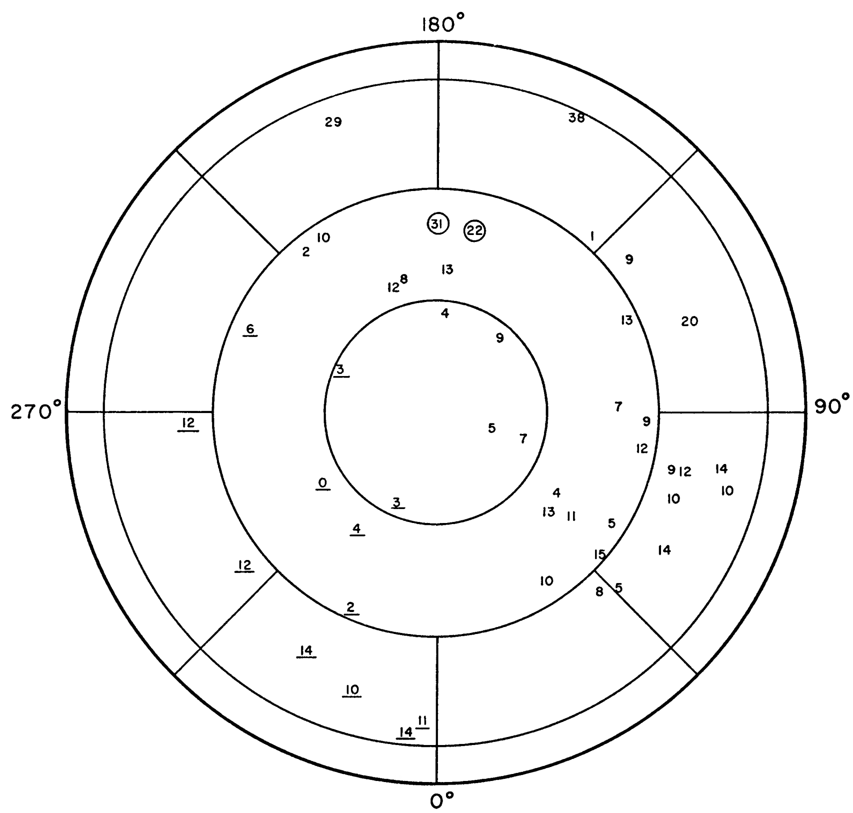

FIG. 14.—The color excess, E_{B-V}, in hundredths of a magnitude for stars in the south galactic hemisphere. The south galactic pole is at the center of the diagram. Latitudes −60°, −30°, and 0° are indicated by concentric circles.

mounting evidence that the reddening at the galactic poles is very small. Kron and Mayall (1960) found from two solutions for the color excess at the galactic poles that $E_{P-V} = 0.052$ and $E_{P-V} = 0.063$ mag. Considering the errors and assumptions involved, these authors felt that their data were in good agreement with the earlier results of Stebbins (1933) and Stebbins and Whitford (1936, 1937) determined from colors of cluster and galaxies. These gave $E_{P-V} = 0.064$ and 0.024 mag. Holmberg (1957) found $E_{B.I} = 0.062$ from the colors of galaxies. These values may be compared to E_{B-V} from the relation

$$E_{P-V} = E_{\mathrm{C.I.}} \simeq 0.8\, E_{B-V} \tag{17}$$

(Kron and Mayall 1960; Morgan, Harris and Johnson 1953). Harris and Upgren (1964) have found an excess of 0.08 mag. in $B - V$ from G stars near the north galactic pole. Klemola (1962), in a study of faint blue stars in this region, found the E_{B-V} could be as large as 0.03 mag. Westerlund (1963) observed bright B and A stars and decided that practically no reddening occurs in the north galactic pole direction, while parts of the southern cap are reddened. Bok and Basinski (1964) have recently found the interstellar reddening in the southern galactic cap to be very small. The value adopted in this paper, $E_{B-V} = 0.03$ mag., seems to be in accordance with the above results.

Recent observations in the infrared have indicated that higher values of A/E than previously determined may be prevalent (Johnson 1965). If this is the case, the apparent disagreement between the absorption inferred from color excesses and that derived from galaxy counts may be resolved. When the relationship between total and selective absorption is understood, the color excesses of RR Lyrae stars can be used to correct their distances for absorption.

b) Stellar Populations

The RR Lyrae stars have long played a prominent role in the study of galactic structure as distance indicators. More recently their importance as population indicators has been recognized. Because of their galactic distribution the variation of chemical composition throughout the whole Galaxy can be studied from these objects.

Studies of this type may be carried out spectroscopically for the solar neighborhood. For the more distant RR Lyrae stars, differences in chemical composition have been inferred rather crudely from period distributions. Now a third means of discriminating population types is at our disposal: the $\delta(U - B)$ parameter.

With the nebular spectrograph of the Crossley reflector, Preston (1959) was able to obtain a spectrogram suitable for determining ΔS in a little less than 1 hour for a star of $m_{\mathrm{pg}} = 13.0$. With the same telescope UBV photometry of the same star can be obtained in 5 min. Thus, by employing wide-band photometry we have gained a factor of 10 in speed with little or no loss in precision.

One immediate result from the $\delta(U - B)$ parameter is obtained in Figure 15 where $\delta(U - B)$ is plotted against period for the stars in this survey. This diagram resembles that of ΔS versus period. Weak-lined stars are noticeably absent shortward of $0^{\mathrm{d}}.44$. The one exception is BK Eri which was discussed earlier. There is a large dispersion in $\delta(U - B)$ at periods slightly longer than $0^{\mathrm{d}}.44$. Small $\delta(U - B)$ values predominate beyond $P = 0^{\mathrm{d}}.50$.

Period-frequency distributions, on a percentage basis, are shown in Figure 16 for various ranges of $\delta(U - B)$. The samples are biased in that stars with $P < 0^{\mathrm{d}}.36$ have been omitted and those with $P \simeq 0^{\mathrm{d}}.5$ were often not observed because it was difficult to obtain observations that were well distributed in phase. The distributions for $\delta(U - B) = 0.00$–0.06 and $\delta(U - B) = 0.06$–0.12 resemble respectively Oosterhoff's Type II and Type I cluster-variable distributions (Oosterhoff 1939). This further confirms evidence that Type I clusters tend to have stronger metallic lines than Type II (Morgan 1956).

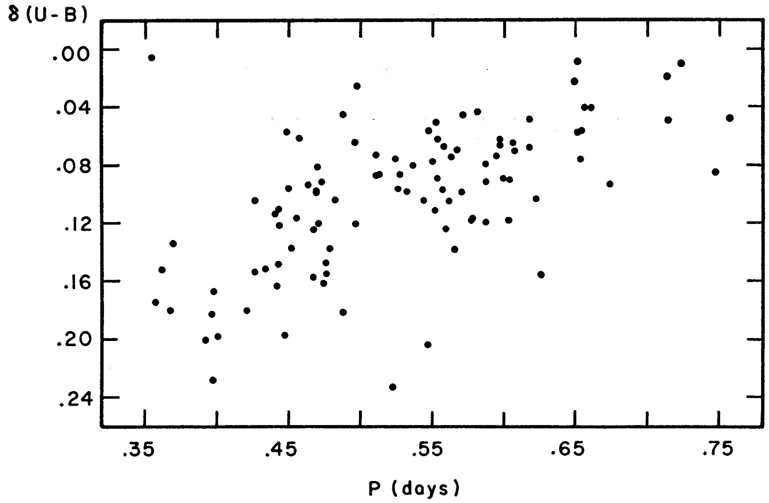

FIG. 15.—The correlation of $\delta(U-B)$ with period

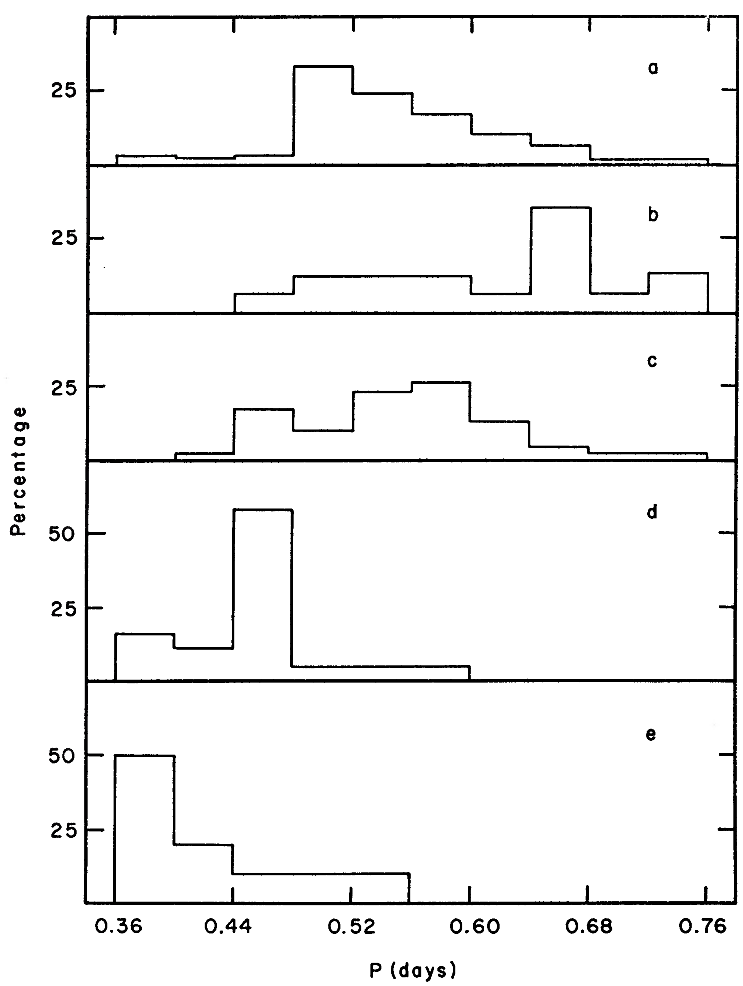

FIG. 16.—Period-frequency diagrams for type *a*, *b* variables. *a*, the distribution for M3; *b*, *c*, *d*, and *e*, the field stars in this survey having $\delta(U-B)$ values of 0.00–0.06, 0.06–0.12, 0.12–0.18, and 0.18–0.24 mag., respectively. The histograms show the percentage of stars found in period intervals of $0^{d}_{.}04$.

c) Globular Clusters

When only $B - V$ colors are known for certain fields or clusters, $\delta(U - B)$ values can be estimated from the period-frequency distribution. The distribution for M3, shown in Figure 16, is taken from Sawyer's (1955) catalogue. It best matches the $\delta(U - B) =$ 0.06–0.12 group.

Dr. A. Sandage has kindly made available to me his $B - V$ color-index–curves for the RR Lyrae stars in M3. The $B - V$'s near minimum light obtained from these data average 0.09 mag. redder than the $(B - V)_c$'s of the field RR Lyrae stars in the galactic cap. If we assume the same color excess for the field stars and M3 ($b = +79°$), the difference in color index would be due to line blanketing. The corresponding value of $\delta(U - B)$ for $\Delta(B - V) = 0.09$ is 0.12 mag.

Both color excess and $\delta(U - B)$ can be obtained directly from the mean $U - B$'s of these variables reported by Sandage (1959). As seen from Figure 2, the mean value of $U - B$ should approximate the value of $U - B$ at minimum light. If this approximation is made, the average $\delta(U - B)$ for the M3 variables is 0.06 and $E_{B-V} = 0.07$ mag. This value is 0.04 mag. larger than the color excess found for the variables in the field.

There is much scatter in these photographic data; the ultraviolet light-curves were obtained by Baker and Baker (1956) at a later epoch. Photoelectric *UBV* photometry of these variables is needed in order to determine precise values of the blanketing and color excess of M3. Only after the color excess is known with accuracy can the age of a globular cluster be determined with accuracy, so such a program for M3 and other clusters with RR Lyrae stars would be of significance.

I wish to express my thanks to Dr. George W. Preston, who suggested this problem and whose ideas and criticisms have been incorporated into all parts of this research. I am indebted to Dr. Charles Perry who allowed me to use his computer program for the reduction of the photoelectric data, and to Dr. Shane and Dr. Sandage for use of their unpublished data. I am grateful to the directors of Lick Observatory and Kitt Peak National Observatory for the observing time, and I also acknowledge the Science and Lick Fellowships of the University of California, held during the course of this study.

REFERENCES

Abt, H. A., and Golson, J. C. 1962, *Ap. J.*, **136**, 363.
Arp, H. C. 1962, *Ap. J.*, **135**, 971.
———. 1965, *ibid.*, **141**, 43.
Baade, W. 1953, *Symposium on Astrophysics* (Ann Arbor: University of Michigan), p. 23.
Baker, R. H., and Baker, H. V. 1956, *A.J.*, **61**, 283.
Bok, B. J., and Basinski, J. 1964, *Mem. Mount Stromlo Obs.*, No. 16.
Eggen, O. J., and Sandage, A. R. 1964, *Ap. J.*, **140**, 130.
Fernie, J. D. 1963, *A.J.*, **68**, 780.
Hardie, R. H. 1955, *Ap. J.*, **122**, 256.
Harris, D. L., and Upgren, A. R. 1964, *Ap. J.*, **140**, 151.
Holmberg, E. 1957, *Medd. Lund Obs.*, ser. 2, No. 136.
Johnson, H. L. 1965, *Ap. J.*, **141**, 923.
Johnson, H. L., and Morgan, W. W. 1953, *Ap. J.*, **117**, 313.
Kinman, T. D. 1961, *Roy. Obs. Bull.*, No. 37, 151.
———. 1963, *Ap. J.*, **137** 698.
Klemola, A. R. 1962, *A. J.*, **67**, 740.
Kron, G. E., and Mayall, N. U. 1960, *A. J.*, **65**, 581.
Morgan, W. W. 1956, *Pub. A.S.P.*, **68**, 509.
Morgan, W. W., Harris, D. L., and Johnson, H. L. 1953, *Ap. J.*, **118**, 92.
Oke, J. B., Giver, L. P., and Searle, L. 1962, *Ap. J.*, **136**, 393.
Oosterhoff, P. T. 1939, *Observatory*, **62**, 104.
Paczynski, B. 1963, *Pub. A.S.P.*, **75**, 400.
Plaut, L. 1963, *Galactic Coordinates l^{II} b^{II} of 15504 Variable Stars* (Moscow: Academy of Sciences of the USSR).

Preston, G. W. 1959, *Ap. J.*, **130**, 507.
———. 1961, *ibid.*, **134**, 633.
———. 1964, *Ann. Rev. Astr. and Ap.*, **2**, 23.
Preston, G. W., and Paczynski, B. 1964, *Ap. J.*, **140**, 181.
Sandage, A. R. 1959, *Ap. J.*, **129**, 596.
Sandage, A. R., and Eggen, O. J. 1959, *M.N.*, **119**, 278.
Sawyer, H. B. 1955, *Pub. David Dunlap Obs. 2*, 35.
Searle, L., and Oke, J. B. 1962, *Ap. J.*, **135**, 790.
Shane, C. D. 1964, private communication.
Slettebak, A., Bahner, K., and Stock, J. 1961, *Ap. J.*, **134**, 195.
Spinrad, H. 1961, *Ap. J.*, **133**, 479.
Stebbins, J. 1933, *Proc. Nat. Acad. Sci. U.S.*, **19**, 222.
Stebbins, J., and Whitford, A. E. 1936, *Ap. J.*, **84**, 132.
———. 1937, *ibid.*, **86**, 247.
Stibbs, D. W. N. 1955, *M.N.*, **115**, 323.
Strömgren, B. 1963, *Basic Astronomical Data*, ed. K. Aa. Strand (Chicago: University of Chicago Press), chap. ix.
Sturch, C. R. 1963, unpublished.
Wampler, E. J. 1961, *Ap. J.*, **134**, 861.
Webb, C. J. 1964, *A.J.*, **69**, 442.
Westerlund, B. E. 1963, *M.N.*, **127**, 83.
Williams, E. T. R. 1934, *Ap. J.*, **79**, 404.